HIDDEN MARKOV MODEL BASED SPECTRUM SENSING FOR COGNITIVE RADIO

by

Thao Tran Nhu Nguyen
A Dissertation
Submitted to the
Graduate Faculty
of
George Mason University
In Partial fulfillment of
The Requirements for the Degree
of
Doctor of Philosophy
Electrical and Computer Engineering

Committee:

_____________________ Dr. Brian L. Mark, Dissertation Co-director

_____________________ Dr. Yariv Ephraim, Dissertation Co-director

_____________________ Dr. Janos Gertler, Committee Member

_____________________ Dr. John Shortle, Committee Member

_____________________ Dr. Andre Manitius, Department Chair

_____________________ Dr. Kenneth S. Ball, Dean, Volgenau School of Engineering

Date: _____________________ Spring Semester 2013
George Mason University
Fairfax, VA

Hidden Markov Model Based Spectrum Sensing
for Cognitive Radio

A dissertation submitted in partial fulfillment of the requirements for the degree of Doctor of Philosophy at George Mason University

By

Thao Tran Nhu Nguyen
Master of Science
George Mason University, 2006
Bachelor of Science
George Mason University, 2004

Co-director: Brian L. Mark, Professor
Co-director: Yariv Ephraim, Professor
Department of Electrical and Computer Engineering

Spring Semester 2013
George Mason University
Fairfax, VA

Dedication

This dissertation is dedicated to my parents, Huong and Nghia, my husband, Thuan, and our three beautiful sons, Viet, Thanh, and An.

Acknowledgments

I owe a million thanks and a tremendous debt of gratitude to many people who made this dissertation possible.

I would like to express my gratitude to my advisors, Professor Brian L. Mark and Professor Yariv Ephraim, for being such amazing advisors throughout the development of this dissertation. They have provided me with their in-depth technical knowledge and invaluable research skills. They have always been supportive, flexible, and patient which has sustained me throughout this unforgettable journey. I am much in debt for their time, expertise, and advice as well as their constructive feedback to make this the best possible dissertation. I hope I could in turn pass on the wisdom of research that they have given to me.

I would also like to thank my committee members, Professor Janos Gertler and Professor John Shortle, who have reviewed the dissertation carefully, provided thoughtful suggestions, and challenged me with difficult yet significant questions. I cannot thank Professor Gertler enough for his encouragement, mentoring, and research support throughout my undergraduate, master, and doctoral studies. I would not have journeyed this far without his influence and motivation.

I would like to express my appreciation to all faculty and staff in the Electrical and Computer Engineering (ECE) department for their support, encouragement and candid advice. I will forever treasure the friendships with the students in the Network Architecture and Performance Lab (NAPL).

I would like to express my appreciation to Shared Spectrum Company (SSC) and the U.S. National Science Foundation for their generous support. I would like to thank Dr. Mark McHenry at SSC for making available the spectrum occupancy measurement data, which is an integral part of this dissertation.

Finally, I want to thank my family. I would not have accomplished this milestone without their unconditional love, support, and encouragement. To my parents, Huong Tran and Nghia Nguyen, who instilled in me the values of education and perseverance, are always there for me. To my husband, Thuan Pham, who has given me much needed strength to overcome any obstacles with his unwavering support, I am forever obliged.

Table of Contents

List of Tables

List of Figures

Abstract

HIDDEN MARKOV MODEL BASED SPECTRUM SENSING
FOR COGNITIVE RADIO

Thao Tran Nhu Nguyen, Ph.D.

George Mason University, 2013

Dissertation Co-director: Dr. Brian L. Mark

Dissertation Co-director: Dr. Yariv Ephraim

Cognitive radio is an emerging technology for sensing and opportunistic spectrum access in wireless communication networks. It allows a secondary user to detect under-utilized spectrum of a primary user and to dynamically access the spectrum without causing harmful interference to the primary user. A number of spectrum sensing techniques has been proposed in the literature to identify the state of the primary user in the temporal domain. However, most of these techniques make instantaneous decisions based on current measurement received at the cognitive radio, and they do not consider the transmission pattern of the primary user which can be acquired from past measurements. Thus, sensing performance can be improved by incorporating measurement history into the sensing decision. Moreover, using all available data may enable prediction of the primary user activity, which will allow a cognitive radio to better plan for its spectrum usage.

In this thesis, we utilize both current and past data to improve temporal spectrum sensing performance for cognitive radio. We focus on sensing of a narrowband channel, and assume that the primary user transmission pattern alternates between idle and active states. We assume that time is slotted into sensing intervals. We formulate the temporal spectrum sensing problem in the framework of hidden Markov models (HMMs), in which the primary transmission pattern is modeled by a Markov chain and the signal power levels received at the cognitive radio is presented by a state dependent Gaussian process. Furthermore, we develop a new statistical model, namely hidden bivariate Markov chain model (HBMM), and apply it to spectrum sensing for cognitive radio. The main advantage of using an HBMM, compared to a standard HMM, is that it allows a non-geometric distribution of the dwell time of the primary user in each state. This distribution, called phase-type, is far more general than the geometric dwell time distribution of a standard HMM. We develop an expectation-maximization (EM) algorithm, which extends the Baum re-estimation algorithms for HMMs, for maximum likelihood estimation of the parameter of the HBMM. We also develop an online recursion for estimation and prediction of the state of the cognitive radio channel. We analyze the performance of our proposed approach using both real spectrum occupancy data and simulated data derived from the spectrum measurements. Our numerical results show that the proposed spectrum sensing approach, which uses the new HBMM outperforms earlier approaches which rely on the standard HMM or a simple energy detector. Performance enhancement is especially noted in scenarios with high path loss and strong shadowing effects, which are characterized by low signal to noise ratio.

Chapter 1: Introduction

1.1 Motivation

Due to the rapid growth of applications and services in wireless communications, the demand for access to additional frequency spectrum has been increasing dramatically. Given that almost all frequency spectrum is allocated, responding to the demand has become one of the major challenges in wireless communications. However, various spectrum occupancy measurement surveys, conducted by the Federal Communications Commission (FCC) [16] and Shared Spectrum Company (SSC) [37], have shown that most of the allocated spectrum is either unused or under-utilized. Therefore, spectrum scarcity in wireless communications is believed to be due to the inefficiency of static frequency allocation rather than the heavy usage of the spectrum.

To better utilize the bandwidth, and thus accommodate an ever increasing demand, cognitive radio and dynamic spectrum access have been proposed to solve the above problem. The two terms are often used interchangeably; but cognitive radio refers to a broader paradigm compared to dynamic spectrum access. Cognitive radio, whose concept was first introduced by Mitola [31], is often based on a software radio platform. It is defined as an intelligent wireless communication system that is aware of its environment and uses the methodology of understanding-by-building to learn from the environment and adapt to statistical variations in the input stimuli, with two primary objectives: 1) highly reliable communication whenever and wherever needed, and 2) efficient utilization of the radio spectrum [23]. Dynamic spectrum access, on the other hand, can be viewed as an important application of cognitive radio that allows secondary users to access the available spectrum in an opportunistic way under an interference constraint to the primary users [39]. In cognitive radio terminology, primary users and secondary users are also referred to as licensed users and unlicensed users, respectively.

Since the concept was introduced, a wide range of applications has been developed for cognitive radio and dynamic spectrum access [24]. The Federal Communications Commission (FCC) has adopted rules to allow unlicensed users to utilize white spaces, i.e., spectrum not being used by a licensed service, in the TV bands [15]. Whereas in the neXt Generation (XG) program sponsored by the Defense Advanced Research Projects Agency (DARPA), the dynamic spectrum access technology is used to dynamically redistribute allocated spectrum in military communications networks [38]. Moreover, the cognitive radio has been proposed for other applications such as inter-operability for public safety systems [36], femtocells, smart grid communications, vehicular networks, cooperative relaying and networks, etc. [24]. There are many standards committees, working groups, forums dedicated to the development of the spectrum access technologies including the IEEE Dynamic Spectrum Access Networks (DySPAN) [25], the Wireless Innovation (WInn) forum [45], the Cognitive Wireless Technology (CWT) at Virginia Tech [43], and others.

1.2 Overview of Spectrum Sensing

There are three basic components in dynamic spectrum access consisting of spectrum sensing, networking, and regulatory policy [51]. Among them, spectrum sensing is the most important component, which provides the awareness of the spectrum usage and existence of licensed users in a geographical area [48]. Performance of a sensing algorithm is often characterized by the probability of missed detection P_{miss} and the probability of false alarm P_{fa}. The probability of missed detection P_{miss} is the probability of failing to sense the presence of the primary user, which leads to interference to the primary user. In contrast, the probability of false alarm P_{fa} is the probability of falsely declaring that the primary user is active, which leads to missing a spectrum opportunity for the secondary user [39]. There is always a tradeoff between P_{miss} and P_{fa}, and the optimal operating point is chosen depending on the capability of the cognitive radio node and the sensing requirements of a specific application.

Spectrum sensing with respect to a fixed frequency channel can be considered in both the spatial and temporal domains. In spatial spectrum sensing, the cognitive radio node estimates the location of the primary system, and then adjusts its transmit power so that it causes no harmful interference to the primary system. The spatial sensing technique takes advantage of the attenuation of radio signal, which capitalizes on the geographical distance between the secondary user and primary system. An example of spatial spectrum sensing method can be found in [28]. In temporal spectrum sensing, on the other hand, the cognitive radio node senses the channel for idle time intervals of the primary transmitter and allows a secondary user to temporarily access the channel during such intervals [42]; even if the primary system is in close proximity to the secondary user. Clearly, finding the spectrum opportunity in the temporal domain is practical only if the idle periods of the primary user are long enough. General spectrum occupancy in the 30 MHz - 3 GHz band [16, 37] and bursty transmission measurements in wireless Local Area Networks (WLANs) [18, 40] illustrate that in most cases, sufficient spectrum is available for secondary users to exploit in the time domain. In addition to the spatial and temporal domains, the spectrum opportunity can be discovered using code dimension and angle dimension [48]. The code dimension space exploits the spread spectrum, time or frequency hopping codes; whereas the angle dimension space utilizes the angle of arrivals feature provided in multi-antenna technologies.

1.3 Problem Statement

In this work, we focus on spectrum sensing of a narrowband channel in the temporal domain. More specifically, the cognitive radio node, which is located in the same vicinity of the primary transmitter, operates on the same channel in such a way that it causes no harmful interference to the primary system. The cognitive radio node first senses the activity of the primary transmitter on the channel, and then determines whether to transmit or not. The cognitive radio node only transmits when the primary transmitter is detected as idle;

otherwise, it remains silent during busy periods of the primary user's transmission.

To identify the presence of the primary transmitter, a number of spectrum sensing schemes have been proposed in the literature [48]. Among them, energy detector based sensing is the most common method, due to its low computational and implementation complexities. In energy detection, the cognitive radio node compares its received signal against a sensing threshold, which depends on the noise floor, to determine the transmission state of the primary transmitter. The energy detector does not need any prior knowledge of the primary user's signal and it usually performs poorly in a low signal-to-noise ratio (SNR) environment. If the primary user's signal patterns are known at the cognitive radio node, a more advanced method called waveform-based sensing can be used, which gives better performance than energy-based sensing in terms of sensing sensitivity and reliability [41]. However, both energy-based sensing and waveform-based sensing do not take into account the measurement history when estimating the state of the primary transmitter, and thus, they can be viewed as "memoryless" sensing methods. Lacking the ability to correlate among measurements, these sensing methods are unable to predict future activity of the channel. In [48], the authors argue that in order to minimize interference to primary users while making the most out of the opportunities, cognitive radios should keep track of primary transmission patterns and should make predictions. Also, it is stated in [8] that gathering statistical information about the primary transmission behavior, in an effort to predict when the channel will be idle, will allow a cognitive radio node to better plan for spectrum usage of the spectrum. Moreover, it is shown in [51] that if the observation history is used optimally, approximately 40% improvement is achieved for the throughput of the secondary user.

Responding to the above claims, we consider the problem of using measurement history received at the cognitive radio node to improve the spectrum sensing in the temporal domain. We develop stochastic models to characterize the transmission pattern of the primary transmitter. Building on these models, we introduce estimation and prediction algorithms for the cognitive radio node. The proposed approach allows a cognitive radio node to achieve better channel state estimation and to predict future activity of the primary user.

1.4 Related Work

Using measurement history for modeling and prediction in spectrum sensing is a challenging problem that has received a lot of attention in recent years. A survey of research related to this problem can be found in [48]. In wireless communications, the transmission pattern of the primary user can be classified into two categories: periodic and non-periodic. For the periodic transmission pattern, e.g., patterns usually found in Time Division Multiple Access (TDMA) networks or radar systems, the periodic feature can be extracted by using a cyclostationary detector [8]. On the other hand, to model the non-periodic transmission pattern of the primary user, a more advanced model such as a hidden Markov model (HMM) must be used [8, 24, 48]. Empirical measurements taken in the 928-948 MHz paging band [19] and in 802.11b based wireless Local Area Network (WLAN) [17] have validated a Markovian pattern in the spectrum occupancy of the primary user. Given that primary user transmission patterns are likely to be non-periodic in most of the frequency spectrum bands, we focus our work on HMM-based modeling and prediction.

In the HMM framework, the primary user transmission pattern can be modeled by either a discrete-time Markov chain or a continuous-time Markov chain. In the discrete-time chains, time is divided into slots and the m-step transition probabilities can be written in matrix form and expressed in terms of the one-step *transition* matrix [21]. In continuous-time, the one-step transition matrix is substituted by a matrix called *generator*, which models the changes of state at the times of jumps. It can be easily proved that the state duration of the discrete-time Markov chain is a geometric distribution; whereas, it is exponentially distributed in the continuous-time case. Depending on the user application, a discrete-time or continuous-time Markov chain can be chosen appropriately. Models employing the discrete-time Markov chain are an important class of models that has been used successfully in speech recognition. Similarly, models with continuous-time Markov chain integrated have been applied in other applications such as modeling ion-channel currents [35] or modeling delays and congestion in computer networks [44]. In [44], the continuous-time process was sampled, and the Baum algorithm was applied for estimating its parameter. This approach has some drawbacks which were detailed in [35]. An EM algorithm for estimating the parameter of a continuous-time bivariate Markov chain was recently developed in [27]. When applying these models to the spectrum sensing problem of cognitive radio, we realize that the modeling the primary user activity by using a continuous-time Markov chain only improves the performance when the primary user changes its state within a sensing period of the secondary user. In this work, we assume that the sensing period is much smaller than the average idle and active periods of the primary user; and thus, a discrete-time Markov chain is adequate for this application.

In addition to those models described above, a hidden semi-Markov model, which is considered as an extension to the standard HMM, is often used to model underlying process that has dwell time in each state is not necessarily geometrically distributed. In the hidden semi-Markov model framework, the dwell time can be represented more accurately with an explicit durational distribution. However, this advantage is often hard to exploit since the exact form of that distribution is usually not known in typical applications. An overview of hidden semi-Markov models, including HMMs with explicit durational models, can be found in [47]. In this work, we propose a new model which allows the dwell time distribution in each state to follow a more general class of distributions, i.e., a discrete phase-type distribution. The proposed model may be viewed as an instance of the hidden semi-Markov model. An advantage of the model proposed here is that estimation of its parameter is done through the Baum algorithm, which is significantly simpler than an algorithm for estimating an explicit durational model.

1.5 Thesis Contributions

The main contributions of the thesis are summarized as follows:

- We formulate the spectrum sensing problem in the temporal domain for cognitive radio application in the framework of hidden Markov models (HMMs). We model the transmission pattern of the primary user by a Markov chain, and represent the signal power level received at the cognitive radio node by an observation process. The Markov chain is assumed to have two states which represent the idle (OFF) and active (ON) states of the primary transmitter. Whereas, the observable process is characterized by a state dependent Gaussian process, which takes into account the path loss and log-normal shadowing introduced by the wireless channel. The spectrum sensing problem of measuring the signal level and estimating the status of the primary transmitter now becomes a statistical problem of estimating a hidden state variable from incomplete observations.

- We develop a new statistical model, namely a hidden bivariate Markov chain model, in solving the spectrum sensing problem. The hidden bivariate Markov chain model is an extension of the standard HMM, in which the Markov chain is substituted by a pair of random processes. The first process in the bivariate Markov chain has two states representing the idle and active states of the primary user, while the second process has several states whose number determines the statistical characteristics of the dwell time distribution in each idle/active state. The advantage of employing the bivariate Markov chain is that the dwell time in each state of the primary user can be modeled by a discrete phase-type distribution, which is a mixture, a convolution, or a combination of geometric distributions. This important property allows us to model the transmission pattern of the primary user more accurately.

- We develop an expectation-maximization (EM), which extends the Baum re-estimation algorithms for HMMs, for maximum likelihood (ML) estimation of the parameter of the proposed model. Given the estimate of the model parameter, the dwell time distribution in each state of the primary user can be easily obtained. Moreover, we introduce an online recursion, based on the prediction and filtering recursions in [12], for estimating the states of the primary user at the current time and future time, given an estimate of the model parameter. In most current dynamic spectrum access schemes, the cognitive radio makes channel access decisions based on the state estimate at the current time. If the cognitive radio is equipped with the state predictive information and dwell time distribution, it can make better decisions in order to minimize interference caused to the primary user while maximizing its channel utilization.

- We test the proposed model using real spectrum occupancy data collected by the Shared Spectrum Company [37]. Since the true state sequence associated with the observation sequence of the real data is not available, we simulate the real data using a *high order* hidden bivariate Markov chain model. The parameter estimate of the high order is considered as the true parameter of the real data and it is used to generate training and testing data for further analysis. We use the training data to estimate parameter of a *low order* hidden bivariate Markov chain. Then, we apply the parameter of the low order model into the proposed detection scheme in order to estimate and predict the state of the primary user from the test sequence. We analyze the state estimation performance in terms of the probability of false alarm P_{fa} and the probability of detection P_{d}. On the other hand, we evaluate the state prediction performance in terms of the probability of prediction error P_{pe} for various values of detection threshold γ. Our numerical studies show that when the dwell time in each state of the primary transmitter is not geometrically distributed, employing the hidden bivariate Markov chain model can significantly improve the accuracy of channel state estimation and prediction, especially in scenarios with severe path loss and shadowing effects.

1.6 Thesis Outline

The remainder of the thesis is organized as follows. In Chapter 2, we provide a literature review and compare our proposed approach with related work. In Chapter 3, we give an overview of the real spectrum measurements which will be used to evaluate the performance of our approach. We also formulate the temporal spectrum sensing problem and discuss how the proposed spectrum sensing approach can be applied in a dynamic spectrum access scheme. In Chapter 4, we introduce a hidden Markov model and estimation algorithms that will be served as background for our proposed approach. In particular, we describe the hidden Markov chain observed through a Gaussian channel and present the Expectation Maximization (EM) algorithm, the forward-backward recursions, the Baum re-estimation algorithm, and state estimation and prediction algorithm. In Chapter 5, we describe the hidden bivariate Markov process and discuss its useful properties for spectrum sensing. We also extend the Baum algorithm for estimating the model parameter and show the state estimation and prediction algorithm for the hidden bivariate Markov chain. In Chapter 6, we describe the simulation setup and performance metrics, and then evaluate the proposed model in spectrum sensing applications using data derived from real spectrum measurements. In Chapter 7, we summarize the thesis contributions and provide some concluding remarks. We also discuss future directions that can be extended from our proposed approach.

Chapter 2: Literature Review

A moderate amount of work has been done in applying hidden Markov models (HMMs) to spectrum sensing in the temporal domain. While several researchers focus on modeling the state of the primary user and the output process, others assume the models are available for their applications. In either case, the model parameter is utilized to enhance the channel state estimation, and more importantly, to predict future activity of the primary user in order to dynamically access the available spectrum. In some papers, the terms "state estimation" and "state prediction" are used interchangeably. However, we will use "state estimation" and "state prediction" to denote the estimation of the true state at the current time and the prediction of the true state at a future time, respectively.

In this chapter, we briefly review some of the related work and address the differences compared to the proposed approach. Most of the existing work has shown that, in general, discrete-time HMMs are sufficient for channel modeling. However, advanced models are needed in some applications to better represent the channel occupancy of the primary users.

2.1 Modeling Using Standard Hidden Markov Models

Modeling the spectrum sensing problem using a standard hidden Markov model signifies the state of the primary user is modeled by either a discrete-time or a continuous-time finite-state homogeneous Markov chain while the output process is modeled by either a finite-alphabet or a general-alphabet process. With the finite-alphabet output process, the number of observations observed in each hidden state is finite; and the probability of an observation produced by a particular hidden state is characterized by a probability mass function. On the other hand, with the general-alphabet output process, the number of observations is not necessary finite and its distribution is usually characterized by a probability density function [12].

In [19], empirical measurements taken in the $928-948$ MHz paging band have validated a Markovian pattern in the spectrum occupancy of the primary user. The main objective of this paper is to recover the hidden state sequence given the observation sequence using the Viterbi algorithm. The spectrum sensing problem was formulated using a simple HMP with two hidden states and two observable states. If the primary user is active, the hidden state is assigned to 0; otherwise, it is assigned to 1. The observation in this model is not the received signal power, but rather, it is a binary value of 0 or 1 depending on the power is higher or lower than a defined threshold, respectively. The probabilities of missed detection and false alarm are used in expressing the observation probabilities given the state. This model is quite simple and can not be generalized in many cases due to the dependence on the threshold. Besides, the parameter estimation and the state prediction have not been discussed in details.

In [1], an algorithm called Markov-based channel prediction algorithm is proposed for dynamic spectrum allocation in cognitive radio networks. The algorithm is based on a Markov chain with a finite-state observable process, whose parameter is estimated online using the forward part of the Baum-Welch algorithm. Using the estimated parameter, activity of the primary user is estimated based on the joint probability between the observation sequence and the state. The cognitive radio utilizes the likelihood of the state estimation to make channel access decision. The proposed approach shows significant signal-to-interference (SIR) performance compared to the traditional Carrier Sense Multiple Access (CSMA) based approach, where the cognitive radio identifies an empty channel and operates on it until the primary user's signal is detected. The duration in each state of the primary user is assumed to be Poisson distributed. Although prediction algorithm is mentioned in the paper, only state estimation is actually performed. On the other hand, this approach is only applicable to high SNR scenarios without considering the detection errors in modeling.

A channel status predictor based on a Markov chain with a finite-alphabet observable process was proposed in [34]. The parameter of the model is estimated from the training data using the Baum-Welch algorithm. The observable process has two states, where 1 represents the OFF state while 2 represents the ON state. The work here focuses on predicting m-step channel state using the forward algorithm. Although the formulation of the model is clearly defined, the performance analysis section in this paper is not well presented. Another problem is that periodic patterns were used as inputs to test the performance of the predictor, which diminishes the advantage of using HMM.

In [5], a modified HMM is proposed to predict the channel state of a single primary user in order to minimize the negative impact of response delays caused by hardware platforms. The modified HMM is developed by shifting the time indexes of the underlying state and the observation to include the maximum possible response delay. Instead of using the Baum re-estimation algorithm to estimate the parameter of the proposed model, the authors of [5] estimate the parameter through a simple statistical process over training sequences. The proposed model is then evaluated using real-world Wi-Fi signal collected in an indoor environment. The performance of the proposed approach is improperly compared with another prediction approach, which assumes the predicted state is the same as the current state.

Unlike the above work, in [39], the spectrum sensing problem in the temporal domain is modelled by a discrete-time Markov chain with general-alphabet observable process. Several sequence detection algorithms derived from the Viterbi and forward-backward algorithms were presented to uncover the state sequence of the primary transmitter given the entire observation sequence observed at the cognitive radio node. The proposed detection sequence algorithms incorporate the probabilities of missed detection and false alarm into the schemes through the use of Bayesian cost factors. Part of our work in [32] is similar to [39] in modeling the primary user's transmission pattern and observation statistics. However, instead of focusing on state sequence detection, we concern ourselves with online single state detection. Although the Baum-Welch algorithm was mentioned in the paper, it has not been implemented to estimate the model parameter. Furthermore, the problem of predicting future activity of the primary transmitter has not been considered in this work.

Arguing that slotted transmission assumption may not be valid for some practical systems, in [49], a continuous-time Markov chain is used to model the primary transmission pattern. Thus, the dwell time of each state of the primary user is exponentially distributed. The work in this paper mainly focuses on designing a periodic sensing scheme of a set of primary channels in order to achieve an optimal spectrum access for the secondary user. In this thesis, we only focus on single channel modeling and leave the spectrum access problem for future work.

2.2 Modeling Using Extended Hidden Markov Models

Several researchers have argued that in some applications the channel occupancy of the primary transmitter can not be properly described by a discrete-time or a continuous-time Markov chain. Therefore, it is mandatory to extend the standard hidden Markov model to a more advanced model such that it can accurately capture the statistics yet possess tolerable computation complexity.

In [18], it has been shown that the idle and active periods of the bursty transmissions of a wireless local area network (WLAN) are not geometrically distributed but rather have phase-type distributions. In another paper [17], a generalized Pareto distribution has been used to statistically model the WLAN data. In both cases, a continuous-time semi-Markov process was proposed as a possibly suitable model for this application but no detailed estimation algorithm was provided. The transition probabilities and the dwell time distributions are approximated in a simple way by matching the statistics of the collected data. Since the work here only focuses on modeling the activity of the primary transmitter, the observable process has been eliminated. The idle and active states of the primary transmitter were identified by using either an energy-based detection or a feature-based detection. It is mentioned in [18] that the state prediction of one-step can be utilized by the secondary user to better access the channel, but no procedure or algorithm was given.

In [40], practical primary user's traffic, whose bursty nature is not properly described by a Markovian pattern, was considered for the opportunistic spectrum access in temporal domain. In particular, two source traffic models were investigated for the primary user: peer-to-peer (P2P) and interactive gaming. The work in this paper focuses on designing an optimal spectrum access scheme which maximizes the spectrum utilization of the secondary user while keeping the interference to the primary system below a given threshold. Numerical results have shown that the channel access strategy of the secondary user depends on both the elapsed time of idle period and the characteristics of the primary user traffic. Therefore, it is very important to model the primary traffic accurately. The primary traffic in this paper was not modeled by any hidden Markov model, but instead, by two specific distributions with known parameters.

With a different approach, we propose a bivariate Markov chain to model the transmission pattern of the primary transmitter for cognitive radio application. The state durations of the bivariate Markov chain have a discrete phase-type distribution. The parameter estimation algorithms in our approach are derived from the Baum re-estimation algorithm, which seeks to maximize the likelihood of the observation data.

Chapter 3: Formulation of Spectrum Sensing Problem

3.1 Overview of Spectrum Occupancy Measurements

Depending on the types of primary users and their transmission behavior, selection of the model that best represents the idle and active states may be different. When the transmission pattern tends to be bursty and reaches a steady-state, the idle/active state can be modeled by a Markov process. However, when the transmission pattern is more dynamic and fast varying, the Markov process may not be valid [46]. Studying various transmission patterns of the primary users is beyond the scope of this work. The goal here is to identify channels or bands, which have similar transmission characteristics with our proposed model, and use them as real data for performance evaluation in Chapter 6.

In selecting the real data for this work, we have examined spectrum occupancy measurements collected by Shared Spectrum Company during the first week of September 2009 [37]. The receiver's antenna was located on the rooftop of a building in Vienna, Virginia. The data was collected in the bandwidth from 30 MHz to 3 GHz, which was divided into 32 smaller well-known bands. A spectrum analyzer was used to sweep across all bands until the collection process was terminated. Further details on the equipment setup and measurement results can be found in [37].

As stated in the report and by analyzing the data, we observe that a) some bands have very high measured spectrum occupancy, b) some bands have very low spectrum occupancy, and c) most of the bands have mixed spectrum occupancy. We list the band names that belong to each category as follows:

1. *Very high measured spectrum occupancy bands:*

These spectrum bands were utilized by the primary users most of the time during the collection period. Examining the data, we find some of these bands are

- FM channels ($88-108$ MHz),
- TV channels (i.e., channels $7, 9, 11, 13, 15, 24, 33-36, 38, 40, 42, 46, 48, 50, 55$),
- Special Mobile Radio (SMR)/Cellular/Personal Communications Service (PCS) downlinks ($851-866$ MHz/$869-894$ MHz/$1930-1990$ MHz),
- Advanced Wireless Services (AWS) bands A/E ($2110-2120$ MHz/$2140-2145$ MHz),
- Private Companies ($2182-2184$ MHz),
- Digital Audio Radio Service (DARS) ($2320-2345$ MHz),
- Several channels in Instructional Television Fixed Service (IFTS)/Multipoint Distribution Service (MDS) ($2644-2686$ MHz),
- A number of narrowband channels existed in different bands spreading across the spectrum below 1 GHz.

As an example, we show the spectrum occupancy measurements of the Special Mobile Radio ($851-866$ MHz) and Cellular downlink ($869-894$ MHz) in Fig. 3.1. Note that other neighboring bands are also displayed in Fig. 3.1. In the figure, three plots are shown. The first plot, which is called max-hold plot, represents the maximum power value measured for each frequency during the data collection period. The second plot, which is called waterfall plot, shows frequency occupancy versus time. A frequency is considered occupied when the power measured at that frequency exceeds a specified threshold. The threshold value chosen for each band is determined based on the noise floor for the band of interest. The third plot shows the fraction of time each frequency is occupied. From the second and third plots, it is obvious that the Special Mobile Radio and Cellular downlink bands are being used most of the time by the primary users.

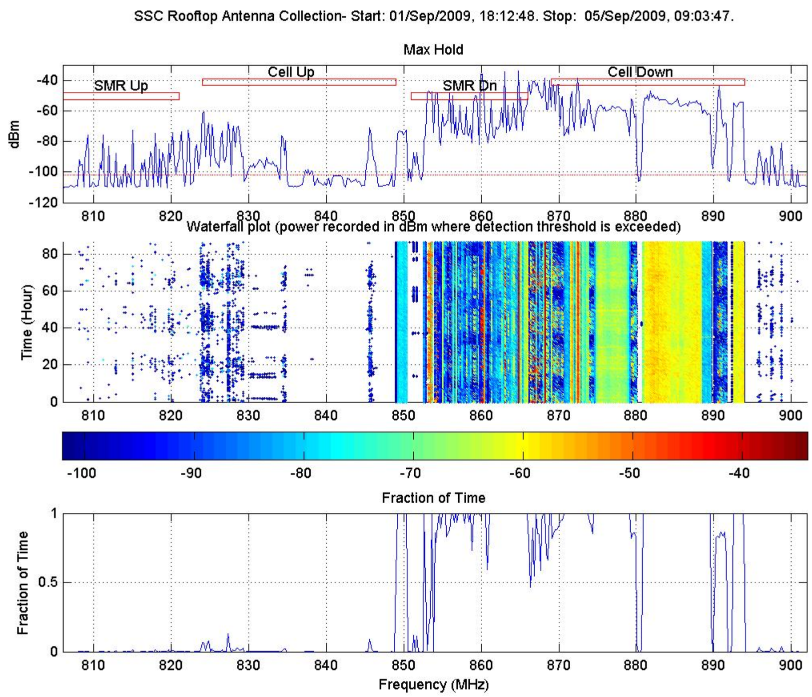

Figure 3.1: Example of very high measured spectrum occupancy band.

Due to their high utilization by the primary users, it is not beneficial for considering these very high measured spectrum occupancy bands for spectrum sharing with secondary users. Therefore, we will exclude these bands from our analysis.

2. *Very low measured spectrum occupancy bands:*

These spectrum bands have either very weak signals, highly under-utilized, or are almost never been used. They include

- TV channels (i.e., channels $8, 10, 12, 16, 19-22, 26, 28, 31, 32, 39, 43, 45, 47, 49, 51-54, 56-60, 65-69$),
- 700 Band Up/Down ($746-764$ MHz/$776-794$ MHz) and Public Safety ($794-806$ MHz),
- Aviation ($960-1020$ MHz), Amateur ($1240-1300$ MHz),

- Military ($1350 - 1390$ MHz), Space/Satellite ($1400 - 1427$ MHz),
- Fixed Mobile ($1432 - 1435$ MHz),
- Telemetry ($1435 - 1525$ MHz and $2360 - 2390$ MHz),
- Mobile Satellite/Meteorological ($1525 - 1710$ MHz),
- Fixed/Fixed Mobile ($1710 - 1850$ MHz),
- Mobile Satellite Service (MSS)/TV Auxiliary ($1990 - 2110$ MHz),
- Space Operation/Fixed ($2200 - 2300$ MHz),
- ITFS/Multichannel Multipoint Distribution Service (MMDS) ($2500 - 2644$ MHz),
- Surveillance Radar ($2700 - 2900$ MHz),
- Weather Radar ($2900 - 3000$ MHz).

Fig. 3.2 shows an example of the very low measured spectrum occupancy bands in the bandwidth of $1400 - 1525$ MHz. As shown in all three plots, the spectrum is almost empty except some very weak signals or noise were observed.

Due to the very low transmit duty cycle, these spectrum bands have great potential for spectrum sharing of cognitive radio. Since these bands are empty most of the time, spectrum sensing for cognitive radio is not an important issue. As a result, we will not consider these bands in our analysis.

3. *Mixed measured spectrum occupancy bands:*

   These spectrum bands have mixed transmit duty cycle ranging from 5% to 95%. Some channels in these bands have long duration of the active state (i.e., in hours) while the others have shorter transmission duration (i.e., in seconds or minutes). Based on the measurement setup, the time resolution of the data is approximately 2 minutes. Therefore, the active state of the primary transmitter could be captured with a single measurement or multiple measurements. In this thesis, we focus on channels that have average idle/active periods greater than 2 minutes. Fig. 3.3 shows an example of the mixed measured spectrum occupancy band in the bandwidth of $928 - 941$ MHz.

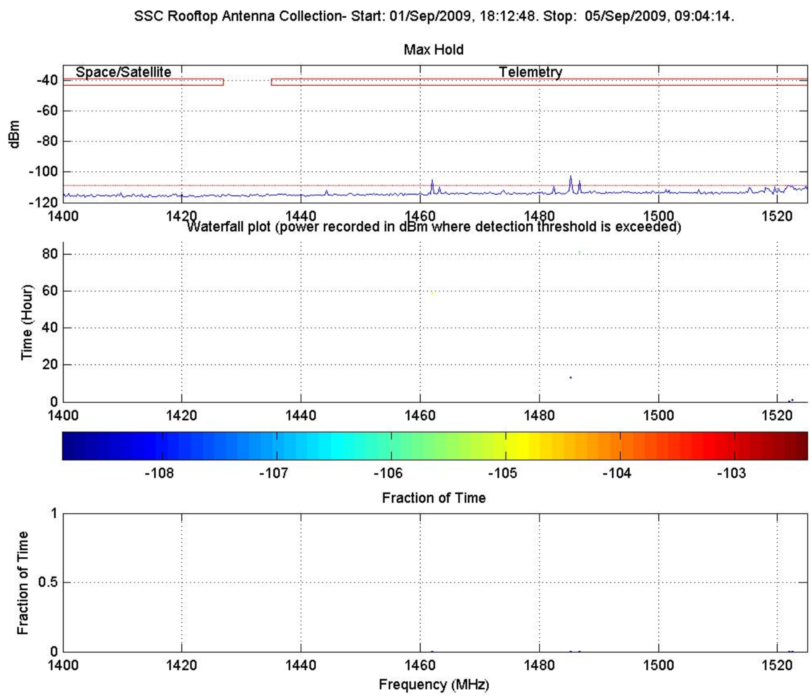

Figure 3.2: Example of very low measured spectrum occupancy band.

We use measurements in the paging band to analyze the performance of our proposed approach. Commercial paging is a Commercial Mobile Radio Service (CMRS), which is provided for profit and available to the public [13]. Traditional commercial paging service consists of one-way data communications sent to a mobile device that alerts the user when it arrives. Narrowband Personal Communication Service (PCS) licensees offer more advanced two-way paging type services. Commercial paging may operate in the $35-36$, $43-44$, $152-159$, and $454-460$ MHz bands, referred to as the "Lower Band", and the 929 and 931 MHz bands, referred to as the "Upper Band". Depending on the band of operation, the channels are either paired or unpaired channels with 20 kHz bandwidth. In our analysis, we focus on channels in the 931 MHz upper band since channels in lower bands have either very low or very high measured spectrum occupancy. We show that the dwell time in each state of the primary transmitter in the paging band is not always geometric distribution

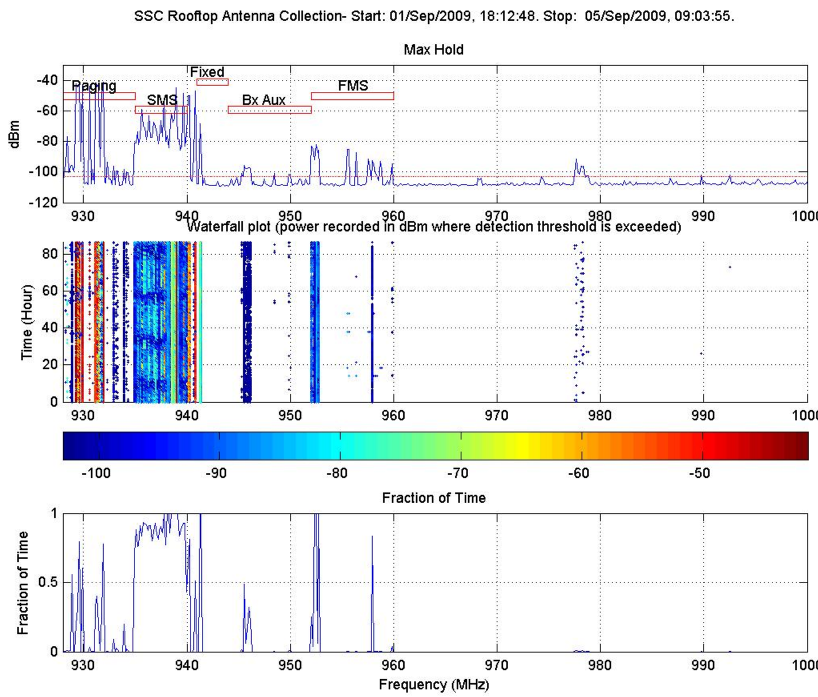

Figure 3.3: Example of mixed measured spectrum occupancy band.

and can be better modeled by a discrete-time phase-type distribution.

3.2 System Model

In this section, we describe the system model for spectrum sensing in cognitive radio. We shall consider a simplified scenario where a single primary transmitter and a single cognitive radio are operating on a single narrowband channel. The primary transmitter is active only when it has data to transmit. The cognitive radio acts as a sensor to determine the state of the primary transmitter. We assume that the locations of the primary transmitter and the cognitive radio are fixed, and the primary transmitter is located within the detection range of the cognitive radio. Fig. 3.4 illustrates the described scenario.

Since the primary user does not fully utilize the designated channel, the channel alternates between idle and active periods of time. The state of the primary transmitter takes

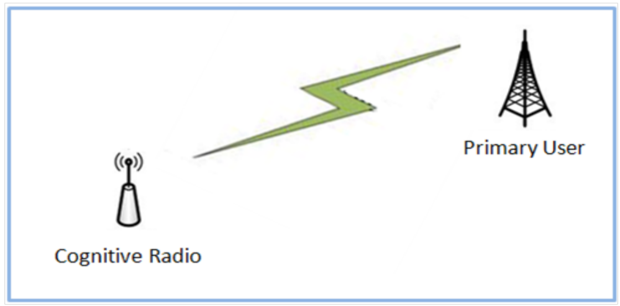

Figure 3.4: Illustration of operation scenario.

values in a finite set $\mathbb{X} = \{1, \dots, d\}$. We shall focus on the case $d = 2$, such that state 1 (also referred to as OFF state) corresponds to the idle state of the primary transmitter, whereas state 2 (also referred to as ON state) corresponds to the active state. Nevertheless, the model and estimation algorithms presented in this thesis will be stated for general values of $d \geq 2$.

We assume that the cognitive radio node senses the channel once every τ seconds. The period τ is assumed to be much smaller than both the average idle period and the average active period of the primary transmitter to ensure the probability that the primary transmitter changes its state within τ is negligible. The state of the primary transmitter can then be represented as a discrete-time random process $\{X_t, t = 0, 1, \dots\}$, where X_t represents the idle/active state of the primary transmitter at time instant t.

We have used a log-distance path loss with shadowing model [29, pp. 40-41] to characterize the wireless propagation environment. Let δ denote the distance from the primary transmitter to the cognitive radio node. The overall log-distance path loss with shadowing $L_p(\delta)$, measured in dB, is given by

$$L_p(\delta) \quad = \quad \left[\bar{L}_p(\delta_0) + 10\kappa \log_{10}\left(\frac{\delta}{\delta_0}\right)\right] + \epsilon_{(dB)}, \quad \delta \geq \delta_0 \tag{3.1}$$

where δ_0 denotes the close-in reference distance, $\bar{L}_p(\delta_0)$ denotes the average log-distance path loss at the reference distance δ_0, κ denotes the path loss exponent, and $\epsilon_{(dB)}$ represents random shadowing effects. The average log-distance path loss $\bar{L}_p(\delta_0)$ is typically calculated using the free space path loss formula or through field measurements. The path loss exponent κ varies for different propagation environments. The random variable $\epsilon_{(dB)}$ is assumed normal with zero-mean and variance σ_ϵ^2.

Let $\{Y_t, t = 0, 1, \ldots\}$ represent the logarithmic power signal, in units of dBm, received at the cognitive radio node. Let $\mathcal{N}(\mu, \sigma^2)$ denote a Gaussian distribution with mean μ and variance σ^2. If Γ denotes the transmit power of the primary user and the distance separating the primary user and the cognitive radio node is $\delta > \delta_0$, then $Y_t \sim \mathcal{N}(\Gamma - \bar{L}_p(\delta), \sigma_\epsilon^2)$, where $\bar{L}_p(\delta) = \bar{L}_p(\delta_0) + 10\kappa \log_{10}\left(\frac{\delta}{\delta_0}\right)$ is the mean path loss at the distance δ. According to (3.1), as δ increases, the path loss $L_p(\delta)$ increases, and thus, the power received at the receiver Y_t decreases.

Fig. 3.5 illustrates the processes $\{X_t\}$ and $\{Y_t\}$ at the primary transmitter and cognitive radio node, respectively. The idle/active state of the primary transmitter X_t at an instant of time t is unknown to the cognitive radio receiver, and thus, it is considered as the hidden or underlying state. Sensing the activity of the primary transmitter at the cognitive radio node is done by measuring the signal level Y_t and estimating the status of the primary transmitter as being active or idle. This formulation is amenable to estimating a state variable from some given noisy and possibly incomplete observations. In addition to the state estimate, utilizing the measurement history at the cognitive radio node allows us to predict future activity of the primary user.

3.3 Dynamic Spectrum Access

In practice, the goal of the cognitive radio node is not only to sense the primary transmitter but also to utilize the available white space. Fig. 3.6 shows a basic slot structure of

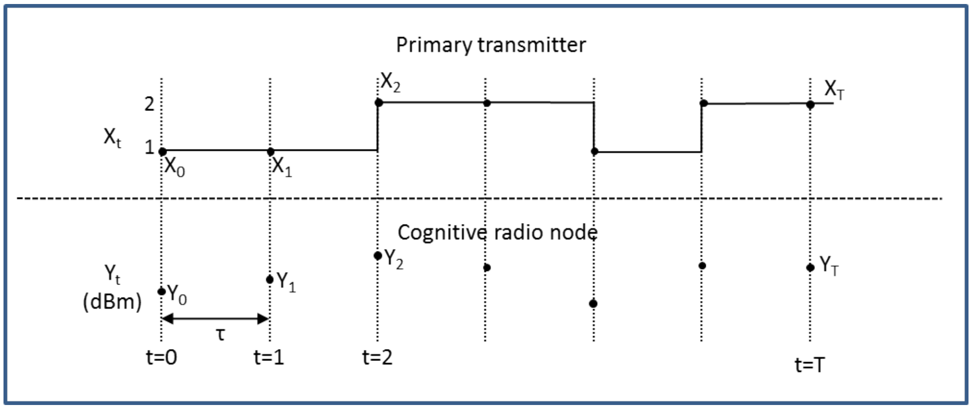

Figure 3.5: Illustration of operation scenario.

the cognitive radio node consisting of the sensing time, the transmission time, and the time dedicated for data transmission acknowledgement. At the beginning of each slot, a secondary user senses the channel and decides to transmit or not based on the sensing outcome. It is assumed that the secondary user always has data to transmit. Given a fixed time slot, the spectrum sensing time and transmission time should be adjusted in order to maximize the throughput of the secondary user while limiting interference to the primary system.

Figure 3.6: Basic slot structure.

In this thesis, we focus on solving the spectrum sensing problem, not the transmission problem, of the cognitive radio. However, we briefly discuss how the proposed state estimation and prediction can be utilized in a dynamic spectrum access scheme for future directions.

The state estimate can be used by a cognitive radio to determine whether or not the channel is occupied by a primary user during the current time slot t. In comparison with an energy detector, which is frequently applied in dynamic spectrum access schemes, the state estimate incorporates knowledge of the behavior of the cognitive radio channel. Under conditions of severe path loss and shadowing effects, we would expect the proposed state estimate to outperform the energy detector in terms of false alarm and detection probabilities, since the energy detector is based only on the received signal at time t.

One of the important features provided by the proposed models is the predictive capability. Given the status of the primary user can be predicted for the next m time slots, the cognitive radio can better prepare for its operation. For example, knowing when the primary user will re-occupy the channel, the cognitive radio can vacate the channel in advance in order to minimize interference caused to the primary user. Using prediction to avoid collisions to the primary system has been investigated in [5, 6, 30]. Conversely, if the cognitive radio seeks to access a given channel, it can predict when the channel will become available and then make preparations to access the channel in advance. This will allow the cognitive radio to make efficient use of the temporal spectrum opportunities on the channel. Several spectrum access schemes that aim to maximize the transmission throughput under interference constraints for the cognitive radio has been developed in [22, 50].

In multi-channel scenario, a cognitive radio often senses a group of N channels simultaneously and selects a best channel to access based on the sensing outcome. It is obvious that the cognitive radio can improve its channel selection process significantly if the dwell time distribution in each state of the primary transmitter is available. Assume that our spectrum sensing approach can be applied to each individual channel. Given the state estimate for each channel at current time t, the cognitive radio may identify $\tilde{N} \leq N$ channels that are available. Instead of randomly choosing a channel from $\tilde{N}$ possible channels for its transmission, the cognitive radio may rank the $\tilde{N}$ channels in decreasing order of the predicted remaining idle time T_{rem} and choose the channel with the largest value of T_{rem}. The remaining $\tilde{N} - 1$ channels can be used as backup channels in case the selected channel is re-occupied by the primary user unexpectedly. On the other hand, if the cognitive radio knows the time T_{acc} it needs to access the channel, it could rank the $\tilde{N}$ channels in decreasing order of the probability that each channel will remain idle at time $t + T_{\text{acc}}$.

In [52], the dynamic spectrum access protocol was developed further in the framework of Partially Observable Markov Decision Process (POMDP). The protocol, which is a cross-layer protocol, integrates spectrum sensing at the physical layer with the spectrum access at the MAC layer and traffic statistics determined by the application layer of the primary network. Due to hardware and energy constraints, it is assumed that the secondary user may not be able to perform full-spectrum sensing or may not be willing to monitor the spectrum when it has no data to transmit. To overcome this problem, both optimal and suboptimal strategies were proposed to assist the secondary user in selecting a set of channels to sense and a set of channels to access based on the sensing outcome. Although we assume the cognitive radio node has the ability to sense a wideband spectrum, which might include more than one channels, our proposed spectrum sensing approach could be integrated in the POMDP framework.

Chapter 4: Background on Hidden Markov Model and Estimation Algorithms

In this chapter, we provide background on the hidden Markov model (HMM) and estimation algorithms. We describe the model and its parameter, and show the dwell time distribution of the underlying process. We then present estimation algorithms related to the model consisting of the Expectation Maximization (EM) algorithm, the forward-backward recursions, the Baum re-estimation algorithms, and the state estimation and prediction algorithm. In the literature, hidden Markov models (HMMs) are also referred to as hidden Markov processes (HMPs) [12]. The two terms will be used interchangeably in this thesis.

4.1 Hidden Markov Model

Markov chains can be defined as a class of random processes possessing a specific form of dependence among current and past samples [20]. A process is called a Markov process if it satisfies the Markov property as follow: *given the present event, future and past events are independent* [21].

An HMM is used to model statistical characteristics of signals that can be described as Markov chains observed through memoryless channels [12]. An HMM is formed by incorporating an observable process with an underlying Markov chain. The underlying Markov chain is said to be *hidden*, and it can be observed only through the observable process. Given the underlying Markov chain, the observed process is conditionally independent.

HMMs consist of a rich family of parametric processes that has been applied in many applications especially in speech recognition. The hidden process can be either discrete-time or continuous-time finite-state homogeneous Markov chain. The output of the observable process can have either finite-alphabet or general-alphabet; and thus, it can be characterized by a probability mass function or a probability density function appropriately. In this chapter, we describe a standard HMM with a discrete-time finite-state Markov chain observed through a time-invariant Gaussian channel. The Gaussian channel is selected for the observable process of this application because it takes into account the wireless channel phenomena such as fading, shadowing, multipath, interference, etc.

In the following subsection, we describe the parameter of the model which consists of an initial state distribution, a transition matrix of the underlying Markov chain, and parameters of the output probability distributions of the observable process. For the Gaussian observable process, the parameters of the output are sets of means and variances.

In this thesis, we use capital letters to denote random variables and lower case letters to denote their realizations. We use the notation v_l^k to denote a sequence $\{v_l, v_{l+1}, \ldots, v_k\}$. We also use the generic notation of $p(\cdot)$ for a density or probability mass function (pmf) as appropriate.

4.1.1 Hidden Markov Model Formulation

A hidden Markov chain with Gaussian densities is a baseline model considered in this thesis. More detail of the model can be found in [12, 32]. The model can be represented as a doubly stochastic process $\{(X_t, Y_t), t = 0, 1, \ldots\}$. The first process $\{X_t\}$ is the hidden process while the second process $\{Y_t\}$ is the observable process. The hidden process $\{X_t\}$ is a discrete-time finite-state homogeneous Markov chain. A chain $\{X_t\}$ is called homogeneous if $P(X_{t+1} = b \mid X_t = a) = P(X_1 = b \mid X_0 = a)$ for all $t = 1, 2, \ldots$ [21]. The number of states of the hidden process constitutes the order of the HMM. The observable process $\{Y_t\}$ is a sequence of conditionally independent random variables given the Markov chain $\{X_t\}$, i.e., the distribution of each random variable Y_t depends on the Markov chain $\{X_t\}$ only through the value X_t at the current time t.

The hidden process $\{X_t\}$ takes values in a finite set $\mathbb{X} = \{1, \ldots, d\}$, where $\mathbb{X}$ is called the *state space* and d denotes the number of hidden states. Let $\pi_a = P(X_0 = a)$, $a \in \mathbb{X}$, denote the probability that the initial state is a. Let $\pi = \{\pi_a, a \in \mathbb{X}\}$ denote a vector representing the initial distribution of $\{X_t\}$. Let $g_{ab} = P(X_{t+1} = b \mid X_t = a), a, b \in \mathbb{X}$ denote the transition probability of $\{X_t\}$ from state a to state b. Let $G = \{g_{ab}, a, b \in \mathbb{X}\}$ denote the $d \times d$ transition matrix of $\{X_t\}$.

For each t, the observation Y_t takes values in an observation space $\mathbb{Y}$. Let $p(y_t \mid x_t)$ denote the probability density function of the observation y_t given the state x_t. The random variables $\{Y_t, t = 0, 1, \ldots\}$ are conditionally independent given $\{X_t, t = 0, 1, \ldots\}$, i.e., for any non-negative integer T,

$$p(y_0^T \mid x_0^T) = \prod_{t=0}^{T} p(y_t \mid x_t). \tag{4.1}$$

We assume, in general, that the observation Y_t is represented by a vector consisting of K components. For any t, $p(y_t \mid x_t)$ is the normal density with mean μ_{x_t} and covariance matrix R_{x_t}. When Y_t is a scalar random variable, then R_{x_t} is referred to as $\sigma^2_{x_t}$ which is the conditional variance of Y_t given x_t. In this work, y_t represents the log-power spectral density of the observed signal. Relying on asymptotic properties of the log-power spectral density estimate [3], we assume that each R_{x_t} is a diagonal matrix. Let $\mu = \{\mu_a, a \in \mathbb{X}\}$ and $R = \{R_a, a \in \mathbb{X}\}$. The hidden Markov chain with Gaussian densities can be represented by a parameter $\phi = (\pi, G, \mu, R)$.

4.1.2 Dwell Time Distribution of HMM

For the Markov chain $\{X_t\}$, the state duration of the dwell-time can be shown to follow a geometric distribution [21]. Let ΔT denote the dwell-time of the underlying state $\{X_t\}$. Then, given the model parameter ϕ and the state a, the probability that the primary transmitter resides in state a for exactly m steps can be computed as:

$$P(\Delta T = m \mid X_t = a) = (g_{aa})^{m-1}(1 - g_{aa}), \quad m = 1, 2, \ldots. \tag{4.2}$$

The expected duration in a state, conditioned on starting in that state can be computed as:

$$E\left[\Delta T \mid X_t = a\right] = \frac{1}{1 - g_{aa}}. \tag{4.3}$$

4.2 EM Algorithm

The Expectation Maximization (EM) is an iterative algorithm that aims to maximize the log-likelihood of a sequence by maximizing the expectation of log-likelihood of another associated sequence. The EM algorithm presented in [10] can be summarized as follows.

In many applications, the underlying state of a model or a process might not be available and only the data samples are observed. The observable data are called incomplete data because they are missing the unobservable data. The set of unobservable and observable data together are called the complete data.

Let X denote the underlying random variable and Y denote the observable random variable. In this case, Y is the incomplete data and (X, Y) is the complete data. Let x and y denote realizations of X and Y, respectively.

Let $p(x; \phi)$ and $p(y; \phi)$ denote the pdf defined on X and Y, respectively, where ϕ is the parameter of the density function. Let $L(y, \phi) = \log p(y; \phi)$ denote the log-likelihood of the observable data. The goal is to find ϕ which maximizes the log-likelihood function $L(y, \phi)$. Unfortunately, the data needed for the computation is not available. The EM algorithm is an iterative algorithm which produces a sequence of estimates with increasing likelihood values.

Suppose that ϕ is a current parameter estimate, and let $\hat{\phi}$ denote a new estimate. Define

$$Q(\phi, \hat{\phi}) = E[\log p(x, y; \hat{\phi}) \mid y; \phi] = \sum_x p(x \mid y; \phi) \log p(x, y; \hat{\phi}), \tag{4.4}$$

$$H(\phi, \hat{\phi}) = E[\log p(x \mid y; \hat{\phi}) \mid y; \phi] = \sum_x p(x \mid y; \phi) \log p(x \mid y; \hat{\phi}), \tag{4.5}$$

where $E[\cdot \mid y; \phi]$ denotes the conditional expectation given $Y = y$ under parameter ϕ.

From (4.4) and (4.5), we have

$$L(y, \hat{\phi}) = Q(\phi, \hat{\phi}) - H(\phi, \hat{\phi}). \tag{4.6}$$

The difference between the two log-likelihoods of the observable data can be expressed as

$$\begin{aligned} L(y, \hat{\phi}) - L(y, \phi) &= Q(\phi, \hat{\phi}) - H(\phi, \hat{\phi}) - [Q(\phi, \phi) - H(\phi, \phi)] \\ &= Q(\phi, \hat{\phi}) - Q(\phi, \phi) + \left[H(\phi, \phi) - H(\phi, \hat{\phi})\right]. \end{aligned} \tag{4.7}$$

From Jensen's inequality [10], we have that $H(\phi, \hat{\phi}) \leq H(\phi, \phi)$. So, if $Q(\phi, \hat{\phi})$ is such that $Q(\phi, \hat{\phi}) \geq Q(\phi, \phi)$, then $L(y, \hat{\phi}) \geq L(y, \phi)$. This implies that the incomplete log-likelihood $L(y, \phi)$ increases monotonically on any iteration of parameter update from ϕ to $\hat{\phi}$, via maximization of the Q-function which is the expectation of log-likelihood of the complete data.

The EM algorithm can be summarized as follows. Given the observed data y and a current estimate ϕ, the new parameter $\hat{\phi}$ can be computed by:

1. E-step. Compute $Q(\phi, \hat{\phi})$ based on the given ϕ.

2. M-step. Choose $\hat{\phi} \in \arg\max_{\hat{\phi}} Q(\phi, \hat{\phi})$. Here, $\arg\max_{\hat{\phi}} Q(\phi, \hat{\phi})$ denotes the set of values $\hat{\phi}$ which maximize $Q(\phi, \hat{\phi})$.

3. Set $\phi = \hat{\phi}$, repeat the process until a stopping criterion is satisfied.

The EM algorithm is terminated when a certain stopping criterion is met, e.g., exceeding maximum number of iterations or when the relative likelihood difference in consecutive iterations falls below a specific value.

4.3 Forward-backward Recursions

The forward-backward recursions were developed for HMMs by Chang and Hancock [4]. They are used to calculate the likelihood of the observed signal, and the conditional probability of a state given the observed process. In addition, the forward-backward recursions can be used to estimate parameters of the Markov processes, as will be shown in the next section. In this section, we describe the forward-backward recursions for the hidden Markov chain with Gaussian densities.

Let $\{y_0^T = y_0, \ldots, y_T\}$ denote the observation sequence for $t = 0, \ldots, T$. Let $\phi = (\pi, G, \mu, R)$ denote the parameter of the model. We define the forward density as:

$$\alpha(x_t, y_0^t) = p(x_t, y_0^t; \phi) \tag{4.8}$$

where y_0^t is the partial observation sequence from time 0 to t. The forward density $\alpha(x_t, y_0^t)$ is the joint probability of the state x_t and the sequence y_0^t given the model ϕ. This probability can be calculated inductively as follows:

Step 1: For $t = 0$, the initial probability is

$$\alpha(x_0, y_0) = \pi_{x_0} p(y_0 \mid x_0). \tag{4.9}$$

Step 2: For $t = 1, \ldots, T$, the forward density $\alpha(x_t, y_0^t)$ can be computed as

$$\alpha(x_t, y_0^t) = \left[\sum_{x_{t-1} \in \mathbb{X}} \alpha(x_{t-1}, y_0^{t-1}) g_{x_{t-1} x_t} \right] p(y_t \mid x_t). \tag{4.10}$$

Step 3: The likelihood of the observation sequence y_0^T is given by

$$p(y_0^T; \phi) = \sum_{x_T \in \mathbb{X}} \alpha(x_T, y_0^T). \tag{4.11}$$

In the above forward iteration, Step 1 initializes the forward densities using the initial probability and density of the observation given the state, for all states at time 0. Step 2 is based on the fact that state x_t can be reached at time t from all the possible states x_{t-1} at time $t-1$. Note that $\alpha(x_{t-1}, y_0^{t-1})$ is the probability of the joint event that the sequence y_0^{t-1} is observed and the last state is x_{t-1}. Thus, the product $\alpha(x_{t-1}, y_0^{t-1})g_{x_{t-1}x_t}$ is the probability that y_0^{t-1} is observed and state x_t is reached through state x_{t-1}. Summing this product over all possible states x_{t-1} results in the probability of state x_t being reached and the observation sequence y_0^{t-1}. Multiplication by $p(y_t \mid x_t)$, which is pdf of the observation y_t given the state x_t, results in $\alpha(x_t, y_0^t)$. Step 3 gives the likelihood of the observation sequence $p(y_0^T; \phi)$ as the sum of the forward densities $\alpha(x_T, y_0^T)$ over all possible states at time T.

Similarly, a backward density can be defined as:

$$\beta(y_{t+1}^T \mid x_t) = p(y_{t+1}^T \mid x_t; \phi) \tag{4.12}$$

where y_{t+1}^T is the partial observation sequence from time $t+1$ to T. The backward density $\beta(y_{t+1}^T \mid x_t)$ is the probability of the partial observation sequence y_{t+1}^T, given state x_t and the model ϕ. This backward density can also be solved inductively in a manner similar to the forward density as follows:

Step 1: For $t = T$, the initial probability is

$$\beta(y_{T+1}^T \mid x_T) = 1. \tag{4.13}$$

Step 2: For $t = T-1, \ldots, 0$, the backward density $\beta(y_{t+1}^T \mid x_t)$ can be computed as

$$\beta(y_{t+1}^T \mid x_t) = \sum_{x_{t+1} \in \mathbb{X}} \beta(y_{t+2}^T \mid x_{t+1}) g_{x_t x_{t+1}} p(y_{t+1} \mid x_{t+1}). \tag{4.14}$$

Step 3: The likelihood of the observation sequence y_0^T is given by

$$p(y_0^T;\phi) = \sum_{x_0 \in \mathbb{X}} \pi_{x_0} p(y_0 \mid x_0)\beta(y_1 \mid x_0). \tag{4.15}$$

For the backward iteration, Step 1 defines the backward density to be 1 for all states at time T. Step 2 shows that in order to have been in state x_t at time t, a transition from state x_t to every state x_{t+1} must be made, which accounts for the observation symbol y_{t+1} given the state x_{t+1} and for the backward density of the remaining observation sequence y_{t+2}^T. Step 3 computes $p(y_0^T;\phi)$ as the sum of the backward densities over all possible states at time 0. The computational complexity of the backward recursion is equivalent to that of the forward recursion.

The forward-backward recursions can be presented in the matrix form as shown in [12, Section V-A]. Let α_t denote the $1 \times d$ vector whose ath element is $\alpha(a, y_0^t), a \in \mathbb{X}$. Let $B(y_t)$ denote an $d \times d$ diagonal matrix whose (a,a) element is $p(y_t \mid X_t = a), a \in \mathbb{X}$. The forward recursion is given by

$$\alpha_0 = \pi B(y_0), \tag{4.16}$$

$$\alpha_t = \alpha_{t-1} G B(y_t), \quad t = 1, \ldots, T. \tag{4.17}$$

Similarly, let β_t denote the $1 \times d$ vector whose ath element is $\beta(y_{t+1}^T \mid a), a \in \mathbb{X}$. Then, the backward recursion is given by

$$\beta_T = \mathbf{1}', \tag{4.18}$$

$$\beta_t = \beta_{t+1} B(y_{t+1}) G', \quad t = T-1, \ldots, 0, \tag{4.19}$$

where $\mathbf{1}$ denotes a $d \times 1$ vector of all ones and $\cdot'$ denotes matrix transpose.

The likelihood of the observation sequence y_0^T can be computed as

$$p(y_0^T;\phi) = \alpha_T \mathbf{1} = \pi B(y_0) \prod_{t=1}^{T} (GB(y_t))\mathbf{1}. \tag{4.20}$$

To improve the numerical stability of the forward-backward recursions, an embedded scaling procedure is implemented [12, Section V-A]. In particular, the forward vector α_t and backward vector β_t are normalized by a factor $c_t = \alpha_t \mathbf{1}$ at each time t. Let $\bar{\alpha}_t$ and $\bar{\beta}_t$ denote the scaled forward vector and the scaled backward vector, respectively. The scaled forward recursion is given by

$$\bar{\alpha}_0 = \frac{\pi B(y_0)}{c_0}, \tag{4.21}$$

$$\bar{\alpha}_t = \frac{\bar{\alpha}_{t-1} GB(y_t)}{c_t}, \quad t = 1, \ldots, T. \tag{4.22}$$

The scaled backward recursion is given by

$$\bar{\beta}_T = \mathbf{1}', \tag{4.23}$$

$$\bar{\beta}_t = \frac{\bar{\beta}(y_{t+1}) B(y_{t+1}) G'}{c_t}, \quad t = T-1, \ldots, 0. \tag{4.24}$$

The computational complexity of the forward and backward recursions is $O(d^2)$ for each step. The scaled and unscaled forward vectors are related by $\bar{\alpha}_t = \alpha_t / \prod_{k=0}^{t} c_k$. The likelihood in (4.20) can be computed in terms of the scaling coefficients as follows:

$$p(y_0^T;\phi) = \alpha_T \mathbf{1} = \left(\prod_{t=0}^{T} c_t \right) \bar{\alpha}_T \mathbf{1} = \prod_{t=0}^{T} c_t. \tag{4.25}$$

Therefore, the log-likelihood is given by

$$\log p(y_0^T; \phi) = \sum_{t=0}^{T} \log c_t. \tag{4.26}$$

4.4 Baum Re-estimation Algorithm

The Baum re-estimation algorithm is the Expectation-Maximization (EM) algorithm described in Section 4.2 when applied to the HMMs. The algorithm was developed and proved to converge by Baum, Petrie, Soules, and Weiss [2]. It is an iterative algorithm that aims to maximize the log-likelihood of a sequence of observations. The new parameter estimate in each iteration is obtained from maximizing an auxiliary function. The maximization process results in re-estimation formulas for the parameter of the model given the observation sequence. In this section, we present the re-estimation equations for the hidden Markov chain with Gaussian densities.

Let $x_0^T = \{x_0, x_1, \ldots, x_T\}$ denote the state sequence of the Markov chain. Let $y_0^T = \{y_0, y_1, \ldots, y_T\}$ denote the sequence of observations. Let $\phi = (\pi, G, \mu, R)$ denote the parameter of the model. The density of y_0^T can be expressed as

$$p(y_0^T; \phi) = \sum_{x_0^T} p(x_0^T, y_0^T; \phi) = \sum_{x_0^T} \prod_{t=1}^{T} g_{x_{t-1}x_t}(\phi) p(y_t \mid x_t; \phi). \tag{4.27}$$

The maximum likelihood estimate $\hat{\phi}$ is obtained as

$$\hat{\phi} = \arg\max_{\phi} \log p(y_0^T; \phi) = \arg\max_{\phi} \log \sum_{x_0^T} p(x_0^T, y_0^T; \phi). \tag{4.28}$$

The Baum algorithm generates a sequence of parameter estimates with nondecreasing likelihood values. Each iteration of the Baum algorithm starts with a current parameter ϕ_ι

and estimates a new parameter $\phi_{\iota+1}$ by maximizing the auxiliary function

$$\sum_{x_0^T} p(x_0^T \mid y_0^T; \phi_\iota) \log p(x_0^T, y_0^T; \phi_{\iota+1}), \tag{4.29}$$

over the parameter ϕ_ι. The algorithm is terminated when a stopping criterion is satisfied, e.g., a maximum number of iterations is executed or when the relative difference of the log-likelihood values in consecutive iterations falls below a given threshold.

Let $p(x_{t-1}, x_t \mid y_0^T; \phi)$ denote the transition probability of $\{X_t\}$ at time $t-1$ to time t given the observation sequence y_0^T for $t = 1, \ldots, T$. Then, the conditional probability can be calculated using the scaled forward and backward densities as follows:

$$p(x_{t-1}, x_t \mid y_0^T; \phi) = \frac{\bar{\alpha}(x_{t-1}, y_0^{t-1})\bar{\beta}(y_{t+1}^T \mid x_t) g_{x_{t-1}x_t} p(y_t \mid x_t)}{\sum_{x_{t-1}, x_t \in \mathbb{X}} \bar{\alpha}(x_{t-1}, y_0^{t-1})\bar{\beta}(y_{t+1}^T \mid x_t) g_{x_{t-1}x_t} p(y_t \mid x_t)}. \tag{4.30}$$

Note that (4.30) can be expressed in the matrix form as follows:

$$p(x_{t-1}, x_t \mid y_0^T; \phi) = \left[\frac{(\bar{\alpha}'_{t-1}\bar{\beta}_t) \odot (GB(y_t))}{\mathbf{1}'[(\bar{\alpha}'_{t-1}\bar{\beta}_t) \odot (GB(y_t))]\mathbf{1}} \right]_{x_{t-1}, x_t}, \tag{4.31}$$

where $\odot$ denotes element-by-element matrix multiplication. Let $p(x_t \mid y_0^T; \phi)$ denote the state probability of $\{X_t\}$ at time t given the observation sequence y_0^T for $t = 1, \ldots, T$. The conditional probability is then given by

$$p(x_t \mid y_0^T; \phi) = \sum_{a \in \mathbb{X}} p(x_{t-1} = a, x_t \mid y_0^T; \phi). \tag{4.32}$$

Let $\hat{\phi} = (\hat{\pi}, \hat{G}, \hat{\mu}, \hat{R})$ denote the new parameter estimate of the hidden Markov chain model obtained during the current EM iteration. In terms of the conditional probabilities in (4.30) and (4.32), the re-estimation formulas are given by

$$\hat{\pi}_a = p(x_0 = a \mid y_0^T; \phi), \tag{4.33}$$

$$\hat{g}_{ab} = \frac{\sum_{t=1}^{T} p(x_{t-1} = a, x_t = b \mid y_0^T; \phi)}{\sum_{b\in\mathbb{X}} \sum_{t=1}^{T} p(x_{t-1} = a, x_t = b \mid y_0^T; \phi)}. \tag{4.34}$$

The estimate parameters of the conditional density $p(y_t \mid x_t = a) = \mathcal{N}(\mu_a, \sigma_a^2), a \in \mathbb{X}$, are given by

$$\hat{\mu}_a = \frac{\sum_{t=0}^{T} p(x_t = a \mid y_0^T; \phi)\ y_t}{\sum_{t=0}^{T} p(x_t = a \mid y_0^T; \phi)}, \tag{4.35}$$

$$\hat{\sigma}_a^2 = \frac{\sum_{t=0}^{T} p(x_t = a \mid y_0^T; \phi)\ (y_t - \hat{\mu}_a)^2}{\sum_{t=0}^{T} p(x_t = a \mid y_0^T; \phi)}. \tag{4.36}$$

For some applications, due to the relatively small numbers involved, the calculation of each summand of the forward-backward formulas and of the probabilities $p(x_{t-1}, x_t \mid y_0^T; \phi)$ is done in the log domain. To ensure the values of $\log p(y_t \mid x_t)$ remain valid, they are shifted into the dynamic range of the computer prior to their summation, simply by replacing the out of range values with the min and max values of the dynamic range.

4.5 State Estimation and Prediction

Suppose that the parameter of the hidden Markov model is $\phi = (\pi, G, \mu, R)$ and that $\{X_t\}$ has two states, i.e., $d = 2$, such that $X_t = 1$ represents the idle state of the primary user while $X_t = 2$ represents its active state. The parameter ϕ is either given or is the estimated parameter. We observe that the conditional probabilities of state X_t given y_0^t is equal to the scaled forward density such as

$$p(x_t \mid y_0^t; \phi) = \bar{\alpha}(x_t, y_0^t), \quad t = 0, \ldots, T. \tag{4.37}$$

Thus, the state probabilities of X_t can be computed recursively using (4.21) and (4.22). More generally, we can compute the conditional m-step predicted state probabilities of X_{t+m} given y_0^t as follows:

$$p(x_{t+m} \mid y_0^t; \phi) = \sum_{x_t} p(x_t \mid y_0^t; \phi) p(x_{t+m} \mid x_t; \phi) = \sum_{x_t} \bar{\alpha}(x_t, y_0^t) \left[G^m\right]_{x_t, x_{t+m}}, \tag{4.38}$$

for $m \geq 0$ and $t \geq 0$. The computational complexity of this forward recursion is $O(md^2)$, or $O(m)$ when $d = 2$.

Let $\hat{X}_{t+m|t}$ denote the m-step predicted state estimate of $\{X_t\}$ at time $t + m$ given y_0^t. When $d = 2$, $\hat{X}_{t+m|t}$ can be determined as follows:

$$\hat{X}_{t+m|t} = \begin{cases} 1, & \text{if } p(x_{t+m} = 1 \mid y_0^t; \phi) \geq \gamma, \\ 2, & \text{otherwise,} \end{cases} \tag{4.39}$$

where $0 < \gamma < 1$ is a decision threshold. By varying γ, a receiver operating characteristic (ROC) curve and prediction curves can be generated. For $\gamma = 0.5$, the m-step predicted state estimate can be computed as follows:

$$\hat{X}_{t+m|t} = \arg\max_{a \in \mathbb{X}} p(x_{t+m} = a \mid y_0^t; \phi). \tag{4.40}$$

Note that the formula (4.40) is also applicable when $d > 2$.

Chapter 5: Hidden Bivariate Markov Chain Model and Estimation Algorithms

As shown in Chapter 4, the dwell time of the hidden state of the hidden Markov model is implicitly a geometric distribution. This causes the hidden Markov model to have limitations in some applications [47]. To overcome this problem, we propose a new model called hidden bivariate Markov chain model, which allows for mixtures, convolutions, or combinations of geometric distributions for the hidden state duration. The model is an extension of a model used for network performance evaluation in [44] by adding the Gaussian observation process to the bivariate Markov process. In this chapter, we describe the proposed model and related estimation algorithms which were developed in details in [33].

5.1 Hidden Bivariate Markov Chain Model

The hidden bivariate Markov chain model can be described as a discrete-time bivariate Markov chain observed through a memoryless Gaussian channel. The bivariate Markov chain is formed by two random processes. The first process is referred to as a *state* process, while the second process is referred to as an *underlying* process. In the spectrum sensing problem, the state process is used to represent the idle and active states of the primary transmitter, and the underlying process is exploited to model the dwell time in each state with a discrete phase-type distribution. The discrete phase-type distribution generalizes the geometric distribution. This important property of the bivariate Markov chain plays a central role in our modeling.

5.1.1 Hidden Bivariate Markov Chain Formulation

Let $\{Z_t = (X_t, S_t), t = 0, 1, \dots\}$ denote a discrete-time, finite-state, homogeneous bivariate Markov chain. We assume that the state process $\{X_t\}$ takes values in $\mathbb{X} = \{1, \dots, d\}$, and the underlying process $\{S_t\}$ takes values in $\mathbb{S} = \{1, \dots, r\}$. The bivariate Markov chain $\{Z_t\}$ takes values in $\mathbb{Z} = \mathbb{X} \times \mathbb{S}$. In the context of spectrum sensing, the process $\{X_t\}$ represents the idle and active states of the primary transmitter and $d = 2$ in this case. The process $\{S_t\}$ affects the distribution of the dwell time of $\{X_t\}$ in each state.

Let $\pi_{a,i} = P(Z_0 = (a, i)) = P(X_0 = a, S_0 = i), a \in \mathbb{X}, i \in \mathbb{S}$, denote the probability that the initial state is (a, i). Let $\pi = \{\pi_{a,i}, a \in \mathbb{X}, i \in \mathbb{S}\}$ denote a $1 \times dr$ vector representing the initial distribution of $\{Z_t\}$. Let $g_{ab}(ij) = P(Z_{t+1} = (b, j) \mid Z_t = (a, i))$ be the transition probability of Z_t from state (a, i) to state (b, j) where $a, b \in \mathbb{X}$ and $i, j \in \mathbb{S}$. Let $G = \{g_{ab}(ij)\}$ denote the $dr \times dr$ transition matrix of $\{Z_t\}$. The transition matrix G can be written as a block matrix $G = \{G_{ab}, a, b \in \mathbb{X}\}$, where $G_{ab} = \{g_{ab}(ij), i, j \in \mathbb{S}\}$ is an $r \times r$ matrix. We assume that G and $\{G_{aa}, a \in \mathbb{X}\}$ are irreducible.

We assume that the bivariate Markov chain $\{Z_t\}$ is observed through a Gaussian memoryless channel with output $\{Y_t\}$. The output process $\{Y_t\}$ takes values in $\mathbb{Y}$, where $\mathbb{Y}$ in general is a subset of $\mathbb{R}$. The observation Y_t represents the signal strength in logarithmic units, i.e., dBm, received at the cognitive radio node. We assume that the observation Y_t depends only on X_t. If Y_t had been assumed to depend on Z_t, then the hidden bivariate Markov chain model would have resulted in a standard HMM with a geometric dwell time distribution in each state of Z_t. In addition, we assume that the random variables $\{Y_t, t = 0, 1, \dots\}$ are conditionally independent given $\{X_t, t = 0, 1, \dots\}$.

Let $p(y_t \mid x_t)$ denote the probability density function of Y_t given X_t. At any time t, $p(y_t \mid x_t)$ is a normal density with mean μ_{x_t} and covariance matrix R_{x_t}. Let $\mu = \{\mu_a, a = 1, \dots, d\}$ and $R = \{R_a, a = 1, \dots, d\}$. The parameter of the hidden bivariate Markov chain model is then given by $\phi = (\pi, G, \mu, R)$.

5.1.2 Dwell Time Distribution of Hidden Bivariate Markov Chain Model

The dwell time distribution of the process $\{X_t\}$ in each of its states can be shown, similar to [27], to be a discrete phase-type distribution. The discrete phase-type distribution can approximate a large class of discrete probability distributions to any desired degree of accuracy [26]. Background on the discrete phase-type distribution is summarized in Appendix A.1. In the remaining of this subsection, we describe how the dwell time distribution in each state of the process $\{X_t\}$ can be computed. Details on the theoretical derivation can be found in [33].

Suppose that the process $\{X_t\}$ jumps at times $T_0 < T_1 < T_2 < \cdots < T_N$ where $T_0 = 0$ and $T_N = T$. For $n = 0, \ldots, N$, define the sampled state chain $\{\tilde{X}_n = X_{T_n}\}$, the sampled underlying chain $\{\tilde{S}_n = S_{T_n}\}$, and the sampled bivariate Markov chain $\{\tilde{Z}_n = Z_{T_n}\}$. For $n = 1, \ldots, N$, let $\Delta T_n = T_n - T_{n-1}$ denote the dwell time of the process in state $\tilde{X}_{n-1}$. By the Markov property of $\{\tilde{Z}_n\}$, we have

$$\begin{aligned} P(\tilde{Z}_{n+1} = z_{n+1}, \Delta T_{n+1} = m \mid \tilde{Z}_n = z_n, \ldots, \tilde{Z}_0 = z_0; T_n = t_n, \ldots, T_0 = t_0) \\ = P(\tilde{Z}_{n+1} = z_{n+1}, \Delta T_{n+1} = m \mid \tilde{Z}_n = z_n) \qquad (5.1) \end{aligned}$$

for any positive integer m. Hence, $\{(\tilde{Z}_n, T_n)\}$ is a discrete-time Markov renewal process. Let $f^{ab}(m) = \{f^{ab}_{ij}(m), i, j = 1, \ldots, r\}$ denote an $r \times r$ matrix with its (i, j) element given by

$$f^{ab}_{ij}(m) = P(\tilde{Z}_1 = (b, j), \Delta T_1 = m \mid \tilde{Z}_0 = (a, i)). \qquad (5.2)$$

It was shown in [33] that

$$f^{ab}(m) = G^{m-1}_{aa} G_{ab}. \qquad (5.3)$$

Let $\tilde{G} = \{\tilde{G}_{ab},\ a, b \in \mathbb{X}\}$ denote the transition matrix of the sampled bivariate Markov chain $\{\tilde{Z}_n\}$. Let I denote the $r \times r$ identity matrix. By summing $f^{ab}(m)$ in (5.3) over all positive integers m we obtain

$$\tilde{G}_{ab} = (I - G_{aa})^{-1} G_{ab}, \qquad a \neq b. \tag{5.4}$$

By definition, $\tilde{G}_{aa}$ is a zero matrix. We assume that $G_{aa}(i,i) > 0$ for all $(a,i) \in \mathbb{Z}$. As shown in [33], we have

$$(I - G_{aa})^{-1} = \sum_{n=0}^{\infty} G_{aa}^{n} > 0. \tag{5.5}$$

Let a row vector ν denote the unique stationary distribution of $\{\tilde{Z}_n\}$, then ν is the unique solution of

$$\nu \tilde{G} = \nu, \qquad \nu \mathbf{1} = 1, \tag{5.6}$$

where $\mathbf{1}$ denotes a column vector of all ones. On the other hand, the stationary probability distribution of $\{Z_t\}$ is given by a row vector π which is the unique solution of

$$\pi G = \pi, \qquad \pi \mathbf{1} = 1. \tag{5.7}$$

The two stationary distributions are related by $\nu \propto \pi \cdot \mathrm{diag}\{(I - G_{11}), \ldots, (I - G_{dd})\}$, see [27].

The following proposition asserts that the conditional dwell time distribution of $\{\tilde{X}_n\}$ in any of its states has a discrete phase-type distribution.

Proposition 1. Define the $1 \times r$ row vector $u_a(n)$ with the ith component given by $P(\tilde{S}_n = i | \tilde{X}_n = a)$. The conditional distribution of ΔT_n given $\tilde{X}_{n-1} = a$ is given by

$$P(\Delta T_n = m \mid \tilde{X}_{n-1} = a) = u_a(n-1) G_{aa}^{m-1} w_a, \qquad m = 1, 2, \ldots, \tag{5.8}$$

where $w_a = \sum_{b:b\neq a} G_{ab}\mathbf{1}$. This is a discrete phase-type distribution with r phases and parameter $(u_a(n-1), G_{aa})$ [26, pp. 47-50].

Proof. We have

$$P(\tilde{Z}_n = (b,j), \Delta T_n = m \mid \tilde{Z}_{n-1} = (a,i)) = f_{ij}^{ab}(m) = \left\{G_{aa}^{m-1} G_{ab}\right\}_{ij}. \tag{5.9}$$

Summing both sides over all $b \neq a$ and over all j, we have

$$P(\Delta T_n = m \mid \tilde{X}_{n-1} = a, \tilde{S}_{n-1} = i) = \left\{ G_{aa}^{m-1} \sum_{b:b\neq a} G_{ab}\mathbf{1} \right\}_i. \tag{5.10}$$

Applying the law of total probability and the definition of w_a, we have

$$P(\Delta T_n = m \mid \tilde{X}_{n-1} = a) = \sum_{i=1}^{r} P(\tilde{S}_{n-1} = i | \tilde{X}_{n-1} = a) \cdot \{G_{aa}^{m-1} w_a\}_i = u_a(n-1) G_{aa}^{m-1} w_a. \tag{5.11}$$

□

5.2 Forward-Backward Recursions

In this section, we describe the forward-backward recursions for the hidden bivariate Markov chain with Gaussian densities model. The recursions are presented in the matrix form. Similar recursions were given in [44].

For $t = 0, \ldots, T$, let $\alpha(z_t, y_0^t)$ denote the forward density of z_t and y_0^t. Define the $d \cdot r$ row vector of such densities as $\alpha_t = \{\alpha((a,1), y_0^t), \ldots, \alpha((a,r), y_0^t), a = 1, \ldots, d\}$. Define an $rd \times rd$ block diagonal matrix $B(y_t)$, with its diagonal blocks given by $\{p(y_t \mid X_t = a)I, a \in$

$\mathbb{X}\}$, where I is an $r \times r$ identity matrix. Then, the forward recursion is given by

$$\alpha_0 = \pi B(y_0), \tag{5.12}$$

$$\alpha_t = \alpha_{t-1} G B(y_t), \quad t = 1, \ldots, T. \tag{5.13}$$

Similarly, let $\beta(y_{t+1}^T \mid z_t)$ denote the backward density of y_{t+1}^T given $Z_t = z_t$. Define the $d \cdot r$ row vector of such densities as $\beta_t = \{\beta(y_{t+1}^T \mid (a, 1)), \ldots, \beta(y_{t+1}^T \mid (a, r)), a = 1, \ldots, d\}$. Then the backward recursion is given by

$$\beta_T = \mathbf{1}', \tag{5.14}$$

$$\beta_t = \beta_{t+1} B(y_{t+1}) G', \quad t = T-1, \ldots, 0, \tag{5.15}$$

where $\cdot'$ denotes matrix transpose. The likelihood of the observed signal is given by

$$p(y_0^T) = \alpha_T \mathbf{1} = \pi B(y_0) \prod_{t=1}^{T} (G B(y_t)) \mathbf{1}. \tag{5.16}$$

Similar to the standard HMM, an embedded scaling procedure is implemented to ensure the numerical stability of the forward-backward recursions. The scaled forward recursion is given by

$$\bar{\alpha}_0 = \frac{\pi B(y_0)}{c_0}, \tag{5.17}$$

$$\bar{\alpha}_t = \frac{\bar{\alpha}_{t-1} G B(y_t)}{c_t}, \quad t = 1, \ldots, T, \tag{5.18}$$

where $c_0 = \pi B(y_0) \mathbf{1}$, and $c_t = \bar{\alpha}_{t-1} G B(y_t) \mathbf{1}$ for $t = 1, \ldots, T$.

The scaled backward recursion is given by

$$\bar{\beta}_T = \mathbf{1}', \tag{5.19}$$

$$\bar{\beta}_t = \frac{\bar{\beta}_{t+1} B(y_{t+1}) G'}{c_t}, \quad t = T-1, \ldots, 0. \tag{5.20}$$

The computational complexity of the forward and backward recursions is $O(d^2 r^2)$, or $O(r^2)$ when $d = 2$, for each step.

The scaled forward $\bar{\alpha}(z_t, y_0^t)$ can be interpreted as the conditional distribution of the process $\{Z_t\}$ given the observable sample path up to time t such as

$$\bar{\alpha}(z_t, y_0^t) = p(z_t \mid y_0^t), \quad t = 0, \ldots, T. \tag{5.21}$$

The scaled and unscaled forward vectors are related by $\bar{\alpha}_t = \alpha_t / \prod_{k=0}^{t} c_k$. The likelihood in (5.16) can be expressed in terms of the scaling coefficients as follows:

$$p(y_0^T) = \alpha_T \mathbf{1} = \left(\prod_{t=0}^{T} c_t \right) \bar{\alpha}_T \mathbf{1} = \prod_{t=0}^{T} c_t. \tag{5.22}$$

Therefore, the log-likelihood is given by

$$\log p(y_0^T) = \sum_{t=0}^{T} \log c_t. \tag{5.23}$$

5.3 Parameter Estimation

We extend the Baum re-estimation algorithm for estimating the parameter of the hidden bivariate Markov chain model in this section, see [33].

Let $z_0^T = \{x_0^T, s_0^T\}$, where $x_0^T = \{x_0, x_1, \ldots, x_T\}$ and $s_0^T = \{s_0, s_1, \ldots, s_T\}$, denote the sequence of the bivariate Markov chain. Let $y_0^T = \{y_0, y_1, \ldots, y_T\}$ denote the sequence of observations. Let $\phi = (\pi, G, \mu, R)$ denote the parameter of the model. The density of y_0^T can be expressed as

$$p(y_0^T;\phi) = \sum_{z_0^T} p(z_0^T, y_0^T;\phi) = \sum_{z_0^T}\prod_{t=1}^{T} g_{z_{t-1}z_t}(\phi)p(y_t \mid x_t;\phi), \tag{5.24}$$

Let $p(z_{t-1}, z_t \mid y_0^T;\phi)$ denote the transition probability of $\{Z_t\}$ at time $t-1$ to time t given the observation sequence y_0^T for $t = 1, \ldots, T$. Then, the conditional probability can be calculated using the scaled forward and backward densities as follows:

$$p(z_{t-1}, z_t \mid y_0^T;\phi) = \frac{\bar{\alpha}(z_{t-1}, y_0^{t-1})\bar{\beta}(y_{t+1}^T \mid z_t)g_{z_{t-1}z_t}p(y_t \mid x_t)}{\sum_{z_{t-1},z_t\in\mathbb{Z}} \bar{\alpha}(z_{t-1}, y_0^{t-1})\bar{\beta}(y_{t+1}^T \mid z_t)g_{z_{t-1}z_t}p(y_t \mid x_t)}. \tag{5.25}$$

The conditional probability can also be expressed in the matrix form as follows:

$$p(z_{t-1}, z_t \mid y_0^T;\phi) = \left[\frac{(\bar{\alpha}'_{t-1}\bar{\beta}_t)\odot(GB(y_t))}{\mathbf{1}'[(\bar{\alpha}'_{t-1}\bar{\beta}_t)\odot(GB(y_t))]\mathbf{1}}\right]_{z_{t-1},z_t}. \tag{5.26}$$

Let $p(z_t \mid y_0^T;\phi)$ denote the state probability of $\{Z_t\}$ at time t given the observation sequence y_0^T for $t = 1, \ldots, T$. The conditional probability is then given by

$$p(z_t \mid y_0^T;\phi) = \sum_{(a,i)\in\mathbb{Z}} p(Z_{t-1} = (a,i), z_t \mid y_0^T;\phi). \tag{5.27}$$

Let $\hat{\phi} = (\hat{\pi}, \hat{G}, \hat{\mu}, \hat{R})$ denote the new parameter estimate of the hidden bivariate Markov chain model obtained during the current iteration. In terms of the conditional probabilities in (5.25) and (5.27), the re-estimation formulas are given by

$$\hat{\pi}_{a,i} = p(z_0 = (a,i) \mid y_0^T; \phi), \tag{5.28}$$

$$\hat{g}_{ab}(ij) = \frac{\sum_{t=1}^T p(z_{t-1} = (a,i), z_t = (b,j) \mid y_0^T; \phi)}{\sum_{(b,j)\in\mathbb{Z}} \sum_{t=1}^T p(z_{t-1} = (a,i), z_t = (b,j) \mid y_0^T; \phi)}. \tag{5.29}$$

When the bivariate Markov chain is observed through a noisy channel with conditional density $p(y_t \mid x_t) = \mathcal{N}(\mu_{x_t}, \sigma_{x_t}^2)$, then the estimate of $\{(\mu_a, \sigma_a^2), a \in \mathbb{X}\}$ is given by

$$\hat{\mu}_a = \frac{\sum_{t=0}^T \sum_{i=1}^r p(z_t = (a,i) \mid y_0^T; \phi)\ y_t}{\sum_{t=0}^T \sum_{i=1}^r p(z_t = (a,i) \mid y_0^T; \phi)}, \tag{5.30}$$

$$\hat{\sigma}_a^2 = \frac{\sum_{t=0}^T \sum_{i=1}^r p(z_t = (a,i) \mid y_0^T; \phi)\ (y_t - \hat{\mu}_a)^2}{\sum_{t=0}^T \sum_{i=1}^r p(z_t = (a,i) \mid y_0^T; \phi)}. \tag{5.31}$$

5.4 State Estimation and Prediction

Suppose that the parameter of the hidden bivariate Markov chain is $\phi = (\pi, G, \mu, R)$ and that $\{X_t\}$ has two states. The parameter ϕ is either given or is the estimated parameter. In this case, the idle and active dwell times of the hidden bivariate Markov chain form a discrete-time alternating renewal process.

The state probabilities of Z_t given y_0^t is simply given by the scaled forward density, i.e.,

$$p(z_t \mid y_0^t; \phi) = \bar{\alpha}(z_t, y_0^t), \quad t = 0, \ldots, T. \tag{5.32}$$

Thus, the state probabilities of Z_t can be computed recursively using (5.17) and (5.18). The conditional m-step predicted state probabilities of Z_{t+m} given y_0^t can be computed as follows:

$$p(z_{t+m} \mid y_0^t; \phi) = \sum_{z_t} p(z_t \mid y_0^t; \phi) p(z_{t+m} \mid z_t; \phi) = \sum_{z_t} \bar{\alpha}(z_t, y_0^t)\, [G^m]_{z_t, z_{t+m}}, \tag{5.33}$$

for $m \geq 0$ and $t \geq 0$. As mentioned above, the complexity of the forward recursion for computing $\bar{\alpha}(z_t, y_0^t)$ is $O(d^2r^2)$ per step. Since G^m can be pre-computed, the computational complexity of the forward recursion (5.33) is also $O(d^2r^2)$, or $O(r^2)$ when $d = 2$. The conditional m-step predicted state probabilities of the bivariate Markov chain X_t given y_0^t are then obtained as follows:

$$p(x_{t+m} = a \mid y_0^t; \phi) = \sum_{i \in \mathbb{S}} p(z_{t+m} = (a, i) \mid y_0^t; \phi), \quad a \in \mathbb{X}, \quad t = 0, \ldots, T. \tag{5.34}$$

Let $\hat{X}_{t+m|t}$ denote the m-step predicted state estimate of $\{X_t\}$ at time $t+m$ given y_0^t. When $d = 2$, $\hat{X}_{t+m|t}$ can be determined as follows:

$$\hat{X}_{t+m|t} = \begin{cases} 1, & \text{if } p(x_{t+m} = 1 \mid y_0^t; \phi) \geq \gamma, \\ 2, & \text{otherwise,} \end{cases} \tag{5.35}$$

where $0 < \gamma < 1$ is a decision threshold. When $\gamma = .5$, this detector implements the maximum a-posteriori (MAP) decision rule for testing whether $\hat{X}_{t+m|t} = 1$ or $\hat{X}_{t+m|t} = 2$ given y_0^t and the estimated parameter ϕ.

Chapter 6: Spectrum Sensing Performance

In this chapter, we study the performance of the proposed approach when applied to spectrum sensing for cognitive radio. Since the HMM is a special case of the hidden bivariate Markov chain model, we will not analyze the performance of the HMM in detail. More information on the HMM and its performance can be found in our earlier work in [32]. Here, we evaluate the performance of the hidden bivariate Markov chain model in general and use the HMM as a special case for comparison purposes. Most of the results presented in this chapter were obtained from [33].

This chapter is organized as follows. In Section 6.1, we describe the simulation setup. In Section 6.2, we discuss the performance metrics that will be used to assess the spectrum sensing performance. Finally, in Section 6.3, we show the numerical results in details.

6.1 Simulation Setup

In this section, we describe the simulation setup that will be used assess the performance of the proposed model. A hidden bivariate Markov chain model with a small value of r is referred to as a *low order* model, while the one with a large value of r is referred to as a *high order* model. Recall that r is the number of states of the underlying chain $\{S_t\}$.

Our approach to spectrum sensing of a cognitive radio channel consists of estimating the parameter of a low order hidden bivariate Markov chain from training data, and incorporating that parameter into the proposed detection scheme in (5.35) in order to estimate and predict the state of the primary user from any given test sequence. In order to be able to assess the performance of this detector, the true state sequence of the channel must be known. Since this sequence is usually not available for real data, we have simulated the real data using a high order hidden bivariate Markov chain. This was done by first estimating the parameter of the high order model from real data obtained from Shared Spectrum Company [37], and then generating training and testing sequences using that parameter. The corresponding state sequences for the simulated data are known.

We separate the analysis into two parts as follows:

1. In the first part, we model the real spectrum measurements using a high order with $d = 2$ and $r = 10$. We apply the parameter estimation algorithm described in Section 5.3 to estimate the parameter of the model. Let $\phi = (\pi, G, \mu, R)$ denote the estimated parameter of the high order hidden bivariate Markov chain. Since the parameter ϕ will be used to generate synthetic data for our subsequent analysis, we will consider ϕ as the true model parameter. Block diagram of this part is depicted in Fig. 6.1.

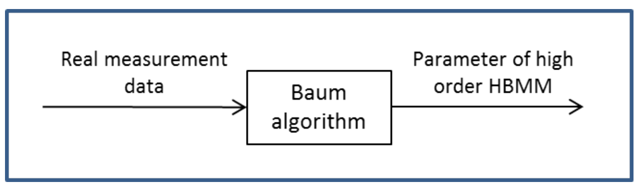

Figure 6.1: Block diagram for channel modeling.

2. In the second part, we evaluate the performance of the low order model for $r = 1, 2, 5$ and $d = 2$ using the synthetic data generated from the parameter ϕ of the high order hidden bivariate Markov chain in part 1. More specifically, the following steps were carried out:

   - We generate training data using the parameter ϕ. Then, we estimate the parameter of the low order hidden bivariate Markov chain from training data. Let $\hat{\phi}$ denote the estimated parameter of the low order hidden bivariate Markov chain. Fig. 6.2 shows the block diagram of this step.

   - We generate test data using the parameter ϕ. We then apply the detection

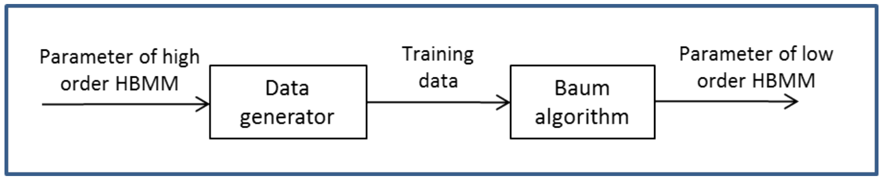

Figure 6.2: Block diagram for the training phase.

scheme in (5.35) to estimate and predict the state of the primary user from the test sequence. Finally, we compare the estimated and predicted states with the true states. Note that the true states associated with the test data is available for the simulated data. Fig. 6.3 shows the block diagram of this step.

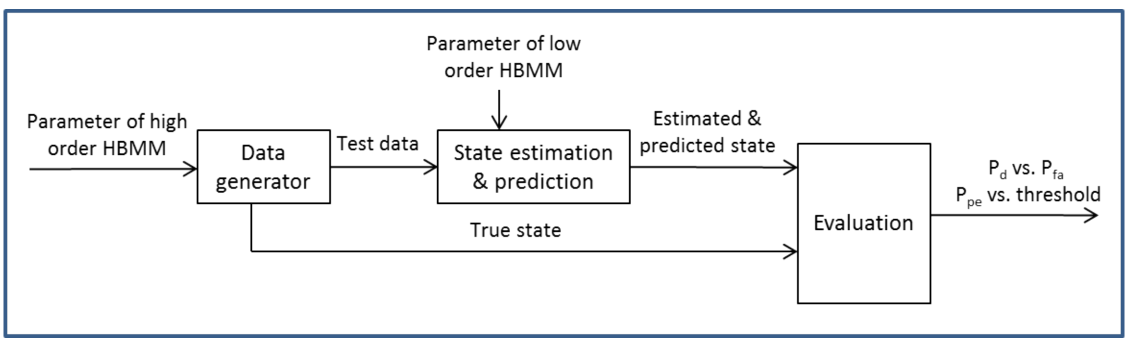

Figure 6.3: Block diagram for testing phase.

For simplicity, we shall ignore the important tradeoff between computational effort and accuracy with respect to spectrum sensing, which is beyond the scope of this work.

6.2 Performance Metrics

In this section, we discuss performance metrics that will be used to assess our proposed detection scheme in (5.35). Let $\phi = (\pi, G, \mu, R)$ denote the parameter of the hidden bivariate Markov chain model. We assume that the process $\{X_t\}$ has two states, i.e., $d = 2$, for which

$X_t = 1$ and $X_t = 2$ represent the idle state and active state of the primary user, respectively. Let y_0^t denote the partial sequence observed from time 0 up to t. Let $\hat{X}_{t+m|t}$ denote the m-step predicted state estimate of $\{X_t\}$ at time $t+m$ given y_0^t. The performances of the state estimation and the state prediction are evaluated as follows.

For the state estimation performance, i.e., $m = 0$, we consider two metrics consisting of probability of false alarm P_{fa} and probability of detection P_{d}. The probability of false alarm P_{fa} is defined as the probability that the active state is detected given that the channel is actually idle. On the other hand, the probability of detection P_{d} is defined as the probability that the active state is identified given that the channel is actually active. In particular, these probabilities can be expressed as follows:

$$P_{\mathrm{fa}} = \frac{P(\hat{X}_{t|t} = 2, X_t = 1)}{P(X_t = 1)}, \tag{6.1}$$

$$P_{\mathrm{d}} = \frac{P(\hat{X}_{t|t} = 2, X_t = 2)}{P(X_t = 2)}. \tag{6.2}$$

Another performance metric which is often used interchangeably with probability of detection P_{d} is probability of missed detection P_{miss}. The probability of missed detection P_{miss} is simply the probability of failing to detect the active state of primary user and it can be computed as

$$P_{\mathrm{miss}} = 1 - P_{\mathrm{d}}. \tag{6.3}$$

Obviously, any detection method which provides lowest values of P_{fa} and P_{miss} (or highest P_{d}) is referred. However, there is always a trade-off between P_{fa} and P_{miss} depending on selection of the decision threshold γ. In the IEEE 802.22 standard, P_{fa} and P_{miss} are required to be smaller than 0.1 for both Wireless Microphones and TV detections [9]. Since avoiding harmful interference to the primary user is more important than utilizing the channel in cognitive radio, a higher P_{fa} value is more acceptable than a higher P_{miss} value.

For the state prediction performance, i.e., $m > 0$, we use probability of prediction error P_{pe} as a single metric to access the proposed prediction scheme. The probability of prediction error P_{pe} at mth step can be computed as follows:

$$P_{\text{pe}}(m) = P(\hat{X}_{t+m|t} = 2 \mid X_{t+m} = 1)P(X_{t+m} = 1) + P(\hat{X}_{t+m|t} = 1 \mid X_{t+m} = 2)P(X_{t+m} = 2), \tag{6.4}$$

where $P(\hat{X}_{t+m|t} = 2 \mid X_{t+m} = 1)$ and $P(\hat{X}_{t+m|t} = 1 \mid X_{t+m} = 2)$ are the conditional probabilities of prediction error given idle state and active state; and $P(X_{t+m} = 1)$ and $P(X_{t+m} = 2)$ are the probabilities of idle state and active state, respectively.

In addition to the state estimation and prediction performance, we also analyze the dwell time distributions of the idle and active states of $\{X_t\}$. These distributions are computed directly from the parameter estimate of the proposed model. A hidden bivariate Markov chain model which provides good approximation of the dwell time distributions of the data should provide better state estimation and prediction performance than a less accurate model.

6.3 Numerical Results

In this section, we evaluate the performance of the proposed spectrum sensing approach. We first estimate the parameter of the high order hidden bivariate Markov chain using real spectrum measurement data. Then, we generate synthetic data from the high order model parameter and analyze the performance of the low order hidden bivariate Markov chain based on the synthetic data.

6.3.1 Channel Modeling Using Real Spectrum Measurement Data

We examine spectrum occupancy measurements collected by Shared Spectrum Company [37] in order to select an appropriate data set for our analysis. In particular, we consider measurements in a spectrum band with bandwidth ranging from 928 MHz to 1000 MHz.

There are 500 frequency bins collected in this band. Thus, the frequency resolution of the spectrum measurement is $(1000 - 928) \cdot 1000/500 = 144$ kHz. The measurements in this band were collected at every 137.83 seconds for a duration of 86.835 hours. Therefore, the number of data samples for each frequency bin is $86.835 \cdot 3600/137.83 \approx 2268$. The elevation of the receiver's antenna was 28.96 meters, with latitude of 38.9260 degrees, and longitude of -77.2456 degrees.

Observing the data, we find that most of the channels have geometric dwell time distributions which can be modeled by a simple HMM as in [32]. However, we discover some channels whose dwell time distributions are not geometric and can not be represented accurately by an HMM. In order to demonstrate that our proposed approach can handle these special cases, we will select measurement data from one of these channels for the analysis.

Within the bandwidth of 928 MHz to 1000 MHz, we select the spectrum measurements in the paging band with center frequency of 931.888 MHz. Since the frequency resolution is 144 kHz, the selected spectrum measurements contain all signals that have frequencies in the range of $931.888 - 144/(1000 \cdot 2) = 931.816$ MHz and $931.888 + 144/(1000 \cdot 2) = 931.960$ MHz. By searching the paging database [7], we find only one registered paging tower in the vicinity has an assigned frequency between 931.816 MHz and 931.960 MHz. The paging tower has a call sign KNKI478 located in McLean, Virginia. The elevation of the tower's antenna is 57.6 meters, with 38.9223 degrees latitude and -77.2289 degrees longitude [14]. The assigned frequency for this tower is 931.9375 MHz and the channel bandwidth is 20 kHz. The maximum effective radiated power (ERP) of the transmitter is $\Gamma = 690$ watts. The radius of the associated macro-cell ranges from 1 to 30 km.

Fig. 6.4 shows the spectrum occupancy measurements at the frequency bin centered at 931.888 MHz. The plot shows the received power in dBm versus time in hours. To provide a better view of the idle periods, we plot the first two hours of the measurements in the zoom-out box located at the top of the plot. Fig. 6.5 shows a histogram of the measurements, which can be easily interpreted as representative of two Gaussian pdfs for the signals during idle and active periods of the channel. Since these signals were recorded using highly elevated antennas for the transmitter and receiver, over a line-of-sight path of 1.5044 km, identifying the idle and active periods is trivial, and can be done using a simple energy detector. The threshold for this detector is set based on the noise level of the spectrum band and noise figure of the receiver. This threshold is shown in Fig. 6.5. Applying the energy detector to the data, we identify the idle periods and calculate the empirical distributions of the idle and active dwell time periods. These distributions are shown in Fig. 6.6.

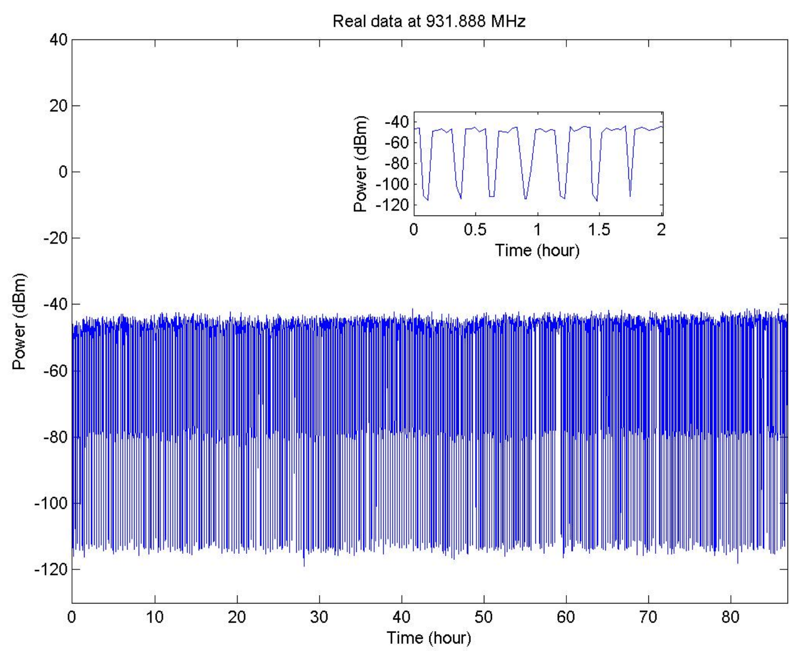

Figure 6.4: Spectrum measurement data from paging band.

We apply the parameter estimation algorithm of Section 5.3 to the spectrum occupancy measurements of Fig. 6.4, in order to estimate the parameter ϕ of the high order hidden bivariate Markov chain with $d = 2$ and $r = 10$ states. We use all available samples of the real data, i.e., $T = 2268$ samples, for this estimation. The algorithm is initialized by a parameter $\phi_{\text{init}} = (\pi_{\text{init}}, G_{\text{init}}, \mu_{\text{init}}, R_{init})$, where π_{init} is a $1 \times dr$ vector with uniformly

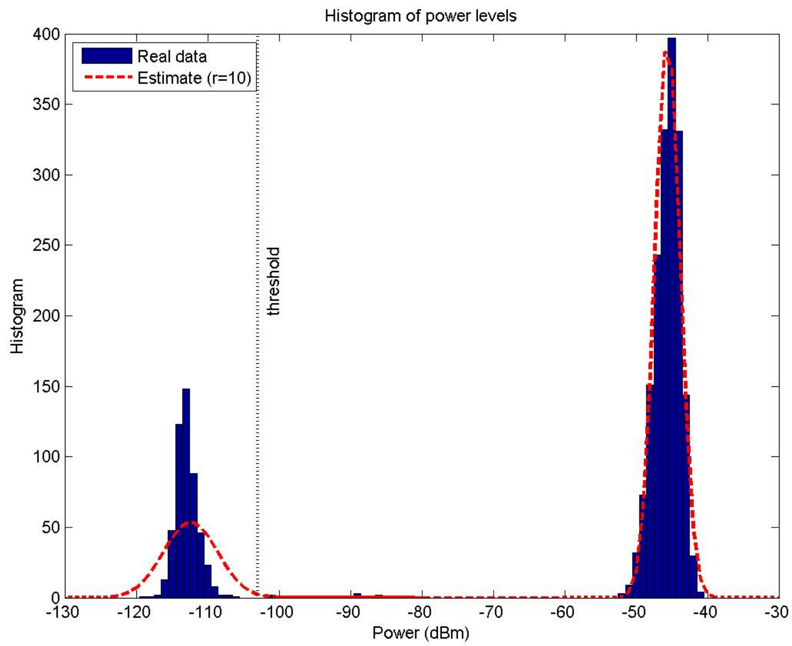

Figure 6.5: Histogram of power levels from paging band data.

distributed elements, G_{init} is a $dr \times dr$ matrix with randomly chosen elements, and

$$\mu_{\text{init}} := (\mu_{1 \text{ init}}, \mu_{2 \text{ init}}) = (-120, -80),$$

$$R_{\text{init}} := (\sigma^2_{1 \text{ init}}, \sigma^2_{2 \text{ init}}) = (5, 5). \tag{6.5}$$

The algorithm is terminated when the relative difference in consecutive log-likelihood values is smaller than 10^{-5} or the number of iterations exceeds 1000.

The estimated initial distribution π is a 1×20 row vector with 19 zero elements and $\pi_{(2,4)} = 1$. The estimated transition matrix G is an 20×20 matrix and is given in Appendix A.2. The estimated means and variances of the two Gaussian output distributions are given

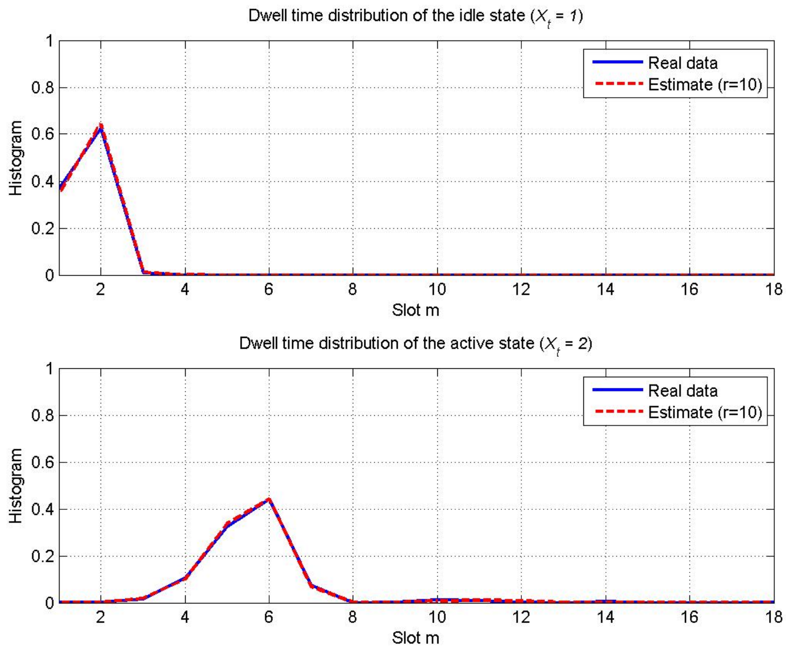

Figure 6.6: Dwell time distributions from paging band data.

by

$$\begin{aligned} \mu &:= (\mu_1, \mu_2) = (-112.4026, -45.6073), \\ R &:= (\sigma_1^2, \sigma_2^2) = (14.2279, 3.1357). \end{aligned} \tag{6.6}$$

The theoretical histogram of power levels generated using the estimated vectors (μ, R) is plotted in Fig. 6.5. While the theoretical histogram of the active state fits the empirical curve very well, the theoretical histogram of the idle state has larger width than the empirical curve. This can be explained by the fact that the estimation algorithm incorporates a few measurements with stronger power level in estimating the parameter associated with the idle state. These unsuitable measurements are interference from adjacent channels or man made noise.

We calculate the dwell time distribution as in (5.8) for the each state of $\{X_t\}$ using the estimated vector (π, G). These distributions are depicted in Fig. 6.6 alongside the empirical dwell time distributions. The empirical and model-based distributions appear to be in good agreement.

6.3.2 Spectrum Sensing Based on Simulated Data

To evaluate the performance of the spectrum sensing scheme proposed in (5.35), we use the parameter ϕ estimated in Section 6.3.1 to generate synthetic data representing the primary user transmission pattern on the channel. We distinguish between two representative cases. In the first case, there exists a line-of-sight between the primary user transmitter and the cognitive radio receiver. We refer to this case as spectrum sensing *under no shadowing*. This situation is the same as the one in which the real spectrum data was obtained. Here, state estimation can be performed accurately with a simple energy detector. However, the energy detector does not provide predictive information; it can only indicate that at the current time the channel is busy, but such an indication may already be too late, as the secondary user cannot instantaneously vacate the channel in practice. Thus, with an energy detector, a secondary user can interfere with the primary user even in the absence of detection errors.

In the second case, we assume that the cognitive radio receiver is located farther away from the primary transmitter. This results in higher path loss and shadowing effects in the reception of the primary signal compared to the real data measurements under no shadowing case. We refer to this case as spectrum sensing *under shadowing effects*. For this situation, we modify the estimated parameter of the conditional Gaussian densities in the high order hidden bivariate Markov chain, and generate new training and testing data. The new training data is used to re-train the low order model, which is then tested on the new testing data. In this case, the simple energy detector may suffer from severe inaccuracy since it does not take the history of the observed data into account. In addition to the prediction performance, we will compare the performance of the energy detector against the model-based detector for the state estimation. We note that the bivariate Markov chain parameter (π, G) for the synthetically generated data is the same in both cases.

Spectrum Sensing: Under No Shadowing

We use the estimated parameter ϕ of the high order hidden bivariate Markov chain to generate training and testing data, from which a low order hidden bivariate Markov chain is estimated and evaluated, respectively. From the initial distribution π and the transition matrix G, a state sequence of the bivariate Markov chain $\{Z_t, t = 0, \ldots, T\}$ is generated, and the state sequence $\{X_t, t = 0, \ldots, T\}$ can be obtained directly from $\{Z_t\}$. The length of the training data is chosen as $T = 2268$, which is similar to the length of the real data. For each state of $\{X_t\}$, an observation y_t is generated which represents the received log-normal power at the cognitive radio node. If the state X_t is idle, i.e., only noise is observed, the received signal sequence is generated from a Gaussian distribution with mean μ_1 and variance σ_1^2; otherwise, when signal in noise is observed, it is generated from a Gaussian distribution with mean μ_2 and variance σ_2^2.

In practical applications, low order models are preferable to reduce the computational overhead but they may result in less accurate modeling of the state dwell time distribution. We estimate three possible orders of the low order hidden bivariate Markov chain given by $r = 1, 2, 5$ using the training data. When $r = 1$ the low order hidden bivariate Markov chain becomes a standard hidden Markov model. This case is studied for comparison purposes. The estimated parameter for $r = 1, 2, 5$ are shown in Tables 6.1, 6.2, and 6.3, respectively. Note that the estimated parameter values of the conditional Gaussian densities are the same in all cases, and they are very close to those values obtained for the high-order model in (6.6).

Next, we use the test data generated from the high order hidden bivariate Markov chain to study the performance of the low order model in detecting the state sequence of the primary user using (5.35). Since the idle and active states can be easily distinguished in this case, state estimation of all models provide excellent performance with P_{fa} and P_{d} close to 0 and 1, respectively.

Fig. 6.7 shows the probability of error, as a function of the threshold γ in (5.35), of the one-step prediction using parameter estimates obtained for $d = 2$ and $r = 1, 2, 5$. We

Table 6.1: Under no shadowing: Parameter estimate for $r = 1$.

Model	Parameter Estimate
HMM (r=1)	$\hat{\pi} = \begin{pmatrix} 0 & 1 \end{pmatrix}$ $\hat{G} = \begin{pmatrix} 0.3869 & 0.6131 \\ 0.1753 & 0.8247 \end{pmatrix}$ $\hat{\mu} = \begin{pmatrix} -112.5603, & -45.6341 \end{pmatrix}$ $\hat{R} = \begin{pmatrix} 13.9720, & 3.0123 \end{pmatrix}$

Table 6.2: Under no shadowing: Parameter estimate for $r = 2$.

Bivariate (r=2)	$\hat{\pi} = \begin{pmatrix} 0 & 0 & 0.9954 & 0.0046 \end{pmatrix}$ $\hat{G} = \begin{pmatrix} 0.0002 & 0.0000 & 0.9998 & 0.0000 \\ 0.6556 & 0.0101 & 0.3343 & 0.0000 \\ 0.0000 & 0.0000 & 0.6498 & 0.3502 \\ 0.0217 & 0.3301 & 0.0001 & 0.6481 \end{pmatrix}$ $\hat{\mu} = (-112.5603, -45.6341)$ $\hat{R} = (13.9720, 3.0123)$

note that there is a significant performance improvement when using the hidden bivariate Markov chain with $r = 2$ compared to using the standard HMM which corresponds to $r = 1$. Improvement is also seen when the order r is increased from 2 to 5. When $r = 5$, the performance is nearly as good as in the case where the high order model, i.e., $r = 10$, is used to detect the state sequence of the primary user. This practically represents the highest achievable performance, since the true parameter used to generate the test data ϕ is applied in detecting the state sequence from this data.

In Fig. 6.8, the performance of m-step prediction for the bivariate model with $r = 5$ is shown. The curves show the probability of prediction error vs. the detection threshold γ for $m = 1, 2, 5, 10$. Consider the special case where $\gamma = 0.5$. We observe that the prediction performances for $m = 1$ and $m = 2$ are similar. However, a major performance degradation is observed when $m = 5$, and especially in the case $m = 10$, as would be expected. Although not shown here, the m-step prediction performance when $r = 2$ is significantly worse than

Table 6.3: Under no shadowing: Parameter estimate for $r = 5$.

Model	Parameter Estimate
Bivariate (r=5)	$\hat{\pi} = \begin{pmatrix} 0 & 0 & 0 & 0 & 0 & 1 & 0 & 0 & 0 & 0 \end{pmatrix}$ $\hat{G}_{11} = \begin{pmatrix} 0.0000 & 0.0000 & 0.0000 & 0.0317 & 0.2679 \\ 0.2049 & 0.0026 & 0.0439 & 0.1771 & 0.2022 \\ 0.0001 & 0.0000 & 0.0000 & 0.2522 & 0.5817 \\ 0.0000 & 0.0000 & 0.0000 & 0.0000 & 0.0000 \\ 0.0000 & 0.0000 & 0.0000 & 0.0000 & 0.0000 \end{pmatrix}$ $\hat{G}_{12} = \begin{pmatrix} 0.0000 & 0.6560 & 0.0444 & 0.0000 & 0.0000 \\ 0.2729 & 0.0859 & 0.0106 & 0.0000 & 0.0000 \\ 0.0001 & 0.0067 & 0.1592 & 0.0000 & 0.0000 \\ 0.0000 & 0.9988 & 0.0012 & 0.0000 & 0.0000 \\ 0.0000 & 1.0000 & 0.0000 & 0.0000 & 0.0000 \end{pmatrix}$ $\hat{G}_{21} = \begin{pmatrix} 0.0000 & 0.0003 & 0.0071 & 0.0000 & 0.0000 \\ 0.0000 & 0.0000 & 0.0000 & 0.0000 & 0.0000 \\ 0.0000 & 0.0000 & 0.0000 & 0.0000 & 0.0000 \\ 0.0003 & 0.0506 & 0.0032 & 0.0000 & 0.0000 \\ 0.0719 & 0.0042 & 0.5823 & 0.1118 & 0.0495 \end{pmatrix}$ $\hat{G}_{22} = \begin{pmatrix} 0.1275 & 0.0000 & 0.0000 & 0.8569 & 0.0082 \\ 0.0032 & 0.1418 & 0.8548 & 0.0003 & 0.0000 \\ 0.8457 & 0.0000 & 0.1346 & 0.0017 & 0.0180 \\ 0.0000 & 0.0000 & 0.0000 & 0.0935 & 0.8524 \\ 0.0000 & 0.0464 & 0.0000 & 0.0000 & 0.1340 \end{pmatrix}$ $\hat{\mu} = \begin{pmatrix} -112.5603, & -45.6341 \end{pmatrix}$ $\hat{R} = \begin{pmatrix} 13.9720, & 3.0123 \end{pmatrix}$

the case of $r = 5$ shown in Fig. 6.8. The best prediction performance is achieved when $r = 10$.

In Fig. 6.9, the dwell time distributions of the process $\{X_t\}$, as calculated from (5.8) using the estimate parameter, corresponding to the low order model with $r = 1, 2, 5$ and the high order model with $r = 10$, are compared. These dwell time distributions are phase-type, as stated in Proposition 1. Clearly, the exponential dwell time distribution of the HMM, which corresponds to $r = 1$, does not provide a good approximation. When $r = 2$, the dwell time distribution in the idle state lines up closely with the distribution corresponding to the high order model, but the dwell time distribution in the active state is very far from that of

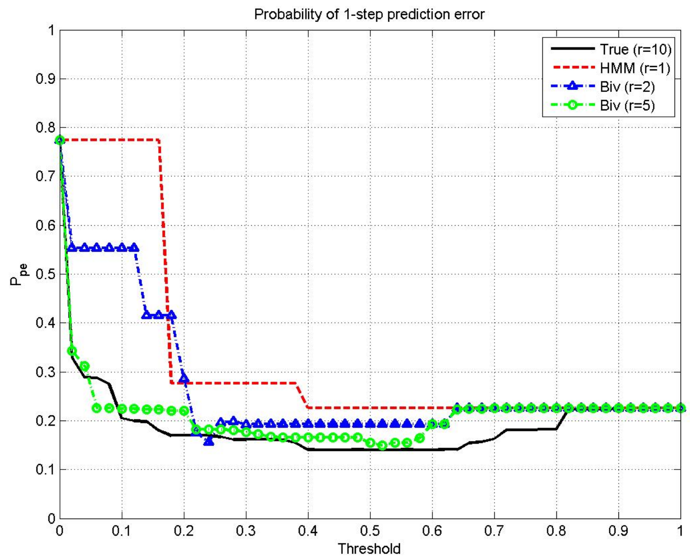

Figure 6.7: Under no shadowing: One-step state prediction performance for $r = 1, 2, 5, 10$.

the high order model. When $r = 5$, the idle state dwell time distribution is indistinguishable from that of the high order model, and a good approximation is obtained for the active state dwell time distribution.

Spectrum Sensing: Under Shadowing Effects

To accommodate the effects of higher path loss and shadowing, we modify the estimated parameter of the high order hidden bivariate Markov chain, and generate new training and testing sequences that are subsequently used to train and test the low order hidden bivariate Markov chain. The means and variances of the conditional Gaussian distributions of the high order model are only affected, while the estimated initial distribution and transition matrix are kept as in the no shadowing case. We ignore fast fading which can be reduced effectively by an averaging filter [29].

We apply the log-distance path loss with shadowing model (3.1) to characterize the wireless propagation environment in this case. We use $\delta = 15$ km for the distance between

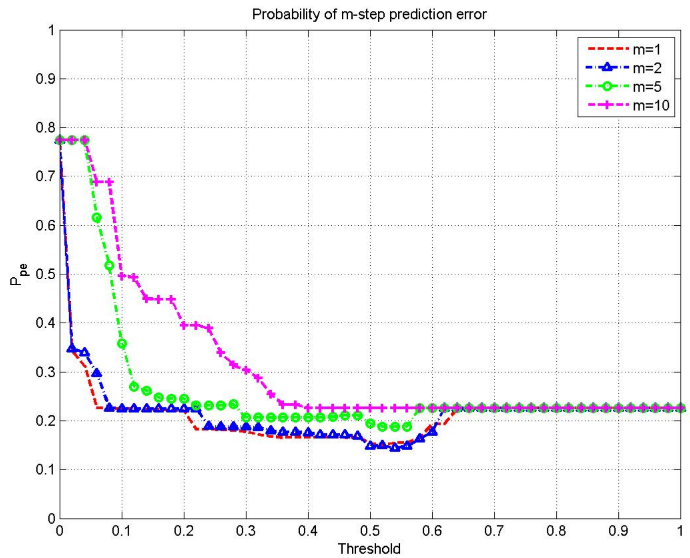

Figure 6.8: Under no shadowing: m-step state prediction performance for $r = 5$ and $m = 1, 2, 5, 10$.

the paging tower and cognitive radio receiver. We set the close-in reference distance $\delta_0 = 1.5044$ km, which is the original distance between the transmitter and receiver under no shadowing case. We set the path loss exponent of $\kappa = 5$ and the standard deviation of the shadowing noise to $\sigma_\epsilon^2 = 64$, which are appropriate values for the shadowed urban area of McLean, Virginia. With these values, $10\kappa \log_{10}\left(\frac{\delta}{\delta_0}\right) = 49.9364$ dB. This loss affects the mean of the received signal Y_t at time t in the active state. Given $\mu_2 = -45.6073$ dBm at distance δ_0 in (6.6), this mean becomes $\mu_2 - 49.9364 = -95.5437$ dBm at distance δ. Thus, the received signal Y_t in the active state in this case is normally distributed with mean -95.5437 dBm, and variance given by $\sigma_2^2 + \sigma_\epsilon^2 = 3.1357 + 64 = 67.1357$. To summarize, the parameter of the conditional Gaussian densities is adjusted from (6.6) to

$$\mu = \{-112.4026,\ -95.5437\}, \quad R = \{14.2279, 67.1357\}, \tag{6.7}$$

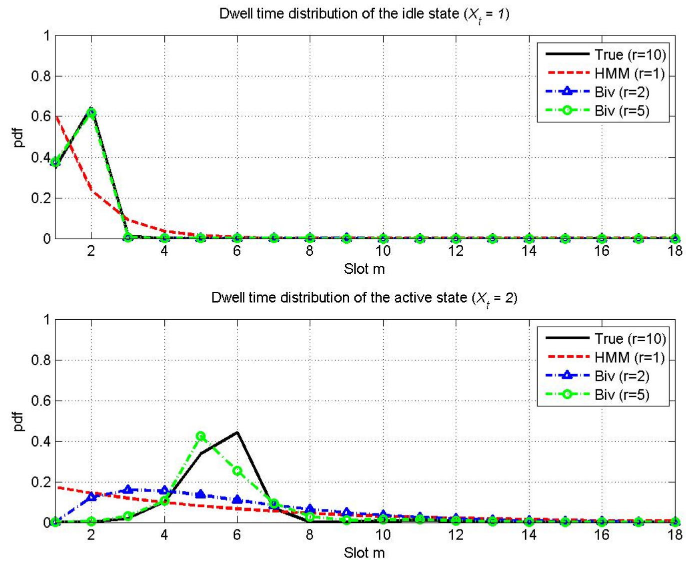

Figure 6.9: Under no shadowing: Inferred dwell time distributions for $r = 1, 2, 5, 10$.

for the modified model, while the parameter of the underlying bivariate Markov chain are kept the same.

Given the modified high order model (6.7), we generate new training data and use it to estimate the low order hidden bivariate Markov chain with $d = 2$ and $r = 1, 2, 5$. The estimated parameter for these models are shown in Tables 6.4, 6.5, and 6.6, respectively. The estimated parameter values of the conditional Gaussian densities vary in three models; but, they are still close to those values in (6.7).

Using the test data generated from the high order model (6.7), we obtain the performance of the low order model. Fig. 6.10 shows ROC curves for state estimation using the energy detector and the hidden bivariate Markov chain model with $r = 1, 2, 5$, and 10. We observe that the HMM-based detector ($r = 1$) performs slightly better than the energy detector. When $r = 2$, the detection performance improves significantly compared to the case $r = 1$. A noticeable improvement is also seen in going from $r = 2$ to $r = 5$. The improved performance with increasing value of r can be attributed to more accurate characterization

Table 6.4: Under shadowing effects: Parameter estimate for $r = 1$.

Model	Parameter Estimate
HMM (r=1)	$\hat{\pi} = \begin{pmatrix} 0 & 1 \end{pmatrix}$ $\hat{G} = \begin{pmatrix} 0.3534 & 0.6466 \\ 0.1923 & 0.8077 \end{pmatrix}$ $\hat{\mu} = \begin{pmatrix} -112.4677, & -95.2042 \end{pmatrix}$ $\hat{R} = \begin{pmatrix} 13.7144, & 68.2014 \end{pmatrix}$

Table 6.5: Under shadowing effects: Parameter estimate for $r = 2$.

Bivariate (r=2)	$\hat{\pi} = \begin{pmatrix} 0 & 0 & 1 & 0 \end{pmatrix}$ $\hat{G} = \begin{pmatrix} 0.0008 & 0.8165 & 0.0871 & 0.0956 \\ 0.0172 & 0.0052 & 0.9776 & 0.0000 \\ 0.0000 & 0.0011 & 0.6297 & 0.3692 \\ 0.2886 & 0.0729 & 0.0008 & 0.6377 \end{pmatrix}$ $\hat{\mu} = (-112.2583, -94.9714)$ $\hat{R} = (14.9889, 65.8092)$

of the dwell time distributions via higher order phase-type distributions. We also note that the ROC curve for $r = 5$ is very close to the ROC curve for $r = 10$, which is obtained by using the true parameter for state estimation. Thus, very good performance can be reached with relatively low order HBMM models.

Fig. 6.11 shows the probability of error of the one-step prediction for the low order model with $r = 1, 2, 5$. The performance of the modified high order with $r = 10$ is plotted for comparison purposes. It is observed that the one-step prediction performance of the low order increases as the order r increases. When $r = 5$, the performance is very close to the highest achievable performance which is obtained from the high order model. As we compare Fig. 6.11 with Fig. 6.7, we notice that under shadowing effects, the prediction performance of the low order model has degraded.

Fig. 6.12 shows the performance of m-step prediction for the bivariate model with $r = 5$. Similar to the no shadowing case, the prediction performance decreases as the number of

Table 6.6: Under shadowing effects: Parameter estimate for $r = 5$.

Model	Parameter Estimate
Bivariate (r=5)	$\hat{\pi} = \begin{pmatrix} 0 & 0 & 0 & 0 & 0 & 1 & 0 & 0 & 0 & 0 \end{pmatrix}$ $\hat{G}_{11} = \begin{pmatrix} 0.0006 & 0.7503 & 0.0142 & 0.0007 & 0.0003 \\ 0.0012 & 0.0000 & 0.0002 & 0.0001 & 0.0005 \\ 0.0042 & 0.0604 & 0.0035 & 0.0001 & 0.0021 \\ 0.0006 & 0.3549 & 0.0752 & 0.0009 & 0.0025 \\ 0.0005 & 0.5560 & 0.0068 & 0.0012 & 0.0010 \end{pmatrix}$ $\hat{G}_{12} = \begin{pmatrix} 0.0036 & 0.0157 & 0.1459 & 0.0687 & 0.0001 \\ 0.0000 & 0.0000 & 0.9802 & 0.0177 & 0.0000 \\ 0.0000 & 0.0160 & 0.9069 & 0.0067 & 0.0001 \\ 0.0146 & 0.1083 & 0.3106 & 0.1315 & 0.0008 \\ 0.0063 & 0.0397 & 0.2670 & 0.1210 & 0.0006 \end{pmatrix}$ $\hat{G}_{21} = \begin{pmatrix} 0.0002 & 0.0000 & 0.0000 & 0.0001 & 0.0001 \\ 0.0000 & 0.0000 & 0.0000 & 0.0000 & 0.0000 \\ 0.0000 & 0.0000 & 0.0000 & 0.0000 & 0.0000 \\ 0.0000 & 0.0000 & 0.0000 & 0.0000 & 0.0000 \\ 0.5414 & 0.0438 & 0.0146 & 0.0691 & 0.1078 \end{pmatrix}$ $\hat{G}_{22} = \begin{pmatrix} 0.0304 & 0.0000 & 0.0002 & 0.0000 & 0.9689 \\ 0.8245 & 0.1521 & 0.0000 & 0.0000 & 0.0234 \\ 0.0227 & 0.0364 & 0.1328 & 0.8082 & 0.0000 \\ 0.0100 & 0.8653 & 0.0001 & 0.1245 & 0.0001 \\ 0.0000 & 0.0000 & 0.0319 & 0.0001 & 0.1913 \end{pmatrix}$ $\hat{\mu} = \begin{pmatrix} -112.4476, & -95.2704 \end{pmatrix}$ $\hat{R} = \begin{pmatrix} 14.5121, & 69.0175 \end{pmatrix}$

steps m increases. Comparing Fig. 6.8 with Fig. 6.12, we again observe a small degradation in the prediction performance under the shadowing effects case.

In Fig. 6.13, we show the dwell time distributions obtained from the estimate parameter of the low order model with $r = 1, 2, 5$ and the high order model with $r = 10$. Similar to the no shadowing case, with higher order r, the dwell time distributions of both idle and active states can be modelled more accurately. Since Fig. 6.9 and Fig. 6.13 are indistinguishable, we conclude that the shadowing effects has little impact on modeling the process $\{X_t\}$ of the bivariate Markov chain.

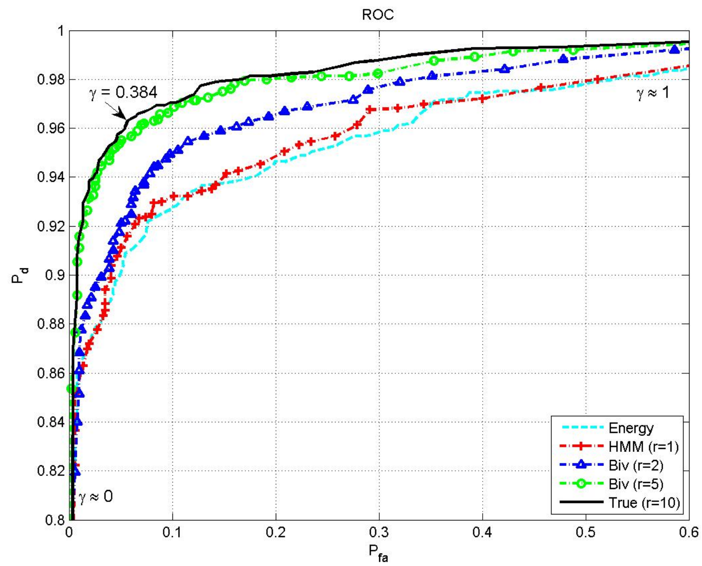

Figure 6.10: Under shadowing effects: State estimation performance for $r = 1, 2, 5, 10$.

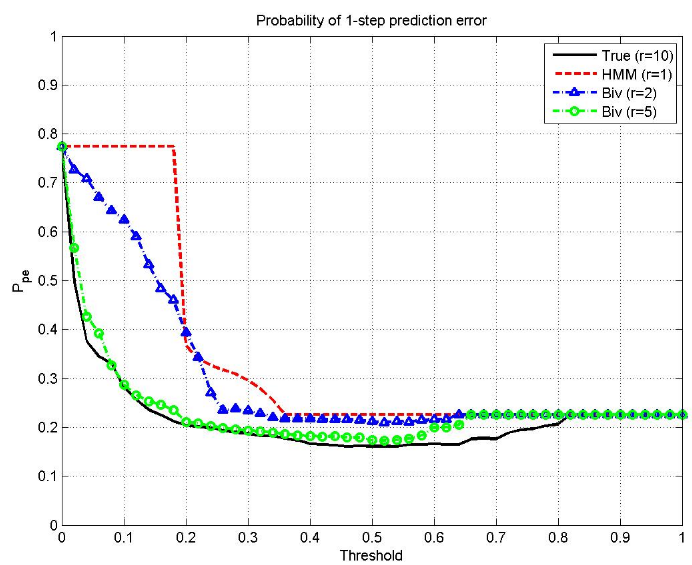

Figure 6.11: Under shadowing effects: One-step state prediction performance for $r = 1, 2, 5, 10$.

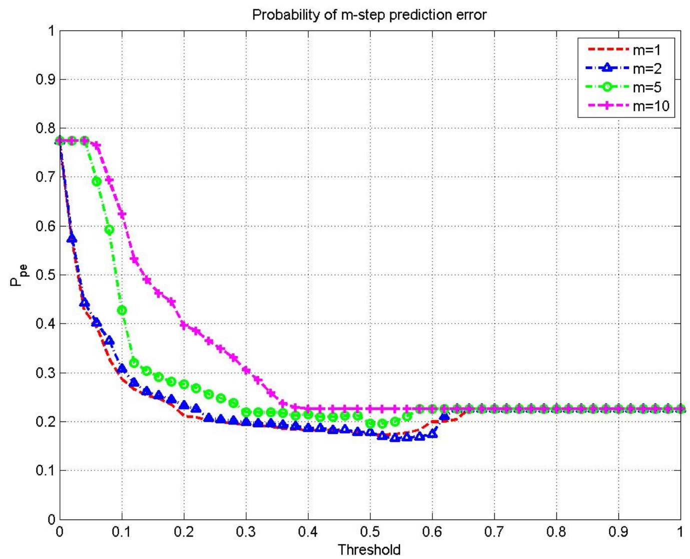

Figure 6.12: Under shadowing effects: m-step prediction performance for $r = 5$ and $m = 1, 2, 5, 10$.

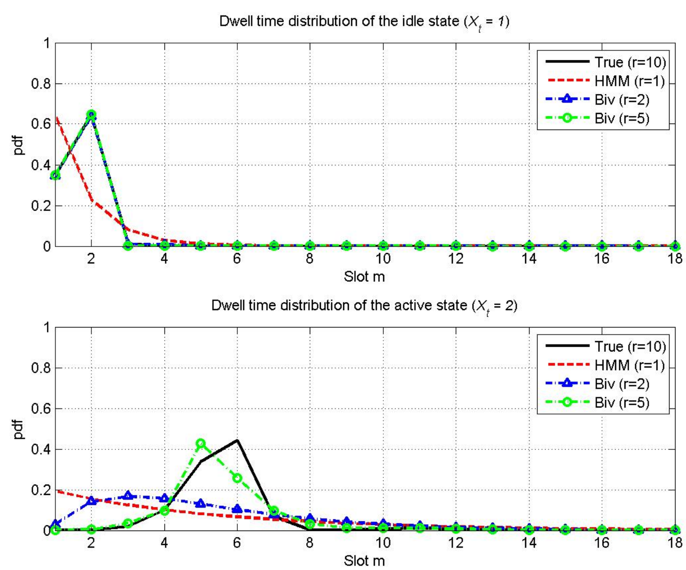

Figure 6.13: Under shadowing effects: Inferred dwell time distributions for $r = 1, 2, 5, 10$.

Chapter 7: Conclusions and Future Directions

The main contribution of this thesis is that the primary transmission pattern can be modeled more accurately by employing the hidden bivariate Markov chain model. In this concluding chapter, we present a summary of the thesis main results followed by a discussion of future research directions.

7.1 Summary

We have formulated the spectrum sensing problem in the temporal domain for cognitive radio application in the HMM framework. We modeled the primary transmission pattern by a Markov chain and represented the signal power levels received at the cognitive radio by Gaussian densities. Although a Markov chain with two states has been a focus in our work, the number of states can be extended to include other possibilities such as *unknown* state (undecided whether the state is idle or active) or a*djacent interference* state, etc. The parameter of the conditional Gaussian densities can be adjusted to accommodate for severe path loss and shadowing effects in certain environments.

We applied the hidden bivariate Markov chain model to the spectrum sensing problem of a narrowband radio signal. The signal was modeled as a bivariate Markov chain observed through a memoryless Gaussian channel. It was shown that using the bivariate Markov chain, the dwell time in each state of the primary user can be modeled by a discrete phase-type distribution, which is more general than the geometric dwell time distribution of a standard HMM.

In the context of spectrum sensing, we developed an EM algorithm for estimating the parameter of the proposed model and applied an online recursion for state estimation and prediction. Given the received signal, the idle/active state of the primary user was estimated using our proposed detection scheme. Prediction of the state of the primary user was also studied in this work. Contrary to a simple energy detector, the proposed approach incorporates the history of the signal in estimating the state at any time instant.

We evaluated the performance of the proposed spectrum sensing approach using both real spectrum measurement data and simulated data derived from the spectrum measurements. Our results for a single narrowband channel showed that the proposed approach leads to more accurate state estimation than a standard HMM or an energy detector, particularly in scenarios with high path loss and/or severe shadowing effects. Also, when the dwell time of each state of the primary user on a given channel is not geometrically distributed, a higher order of the underlying chain results in better state estimation and prediction performance at the expense of greater computation overhead.

7.2 Future Directions

In this thesis, we focused on spectrum sensing of a narrowband channel in the temporal domain for cognitive radio. There are other potential research areas which can be extended from our work.

First of all, enhanced dynamic spectrum access schemes, which allow cognitive radio nodes to utilize the predictive knowledge provided by the proposed model, should be investigated. In a single channel network, the predictive knowledge can be used to overcome the negative impact of response delays caused by hardware platforms. Whereas, in a system with multiple channels, the advanced knowledge enables the cognitive radio network to identify best channels, e.g., channels predicted to remain idle for the longest period of time, for the operation. Overall, the goal is to access the available spectrum more efficiently without causing harmful interference to primary users.

The approach can also be extended to support collaborative spectrum sensing (see, e.g., [11]), whereby the observations of multiple cognitive radio receivers are combined to improve sensing accuracy. In this case, each observation Y_t in the hidden bivariate Markov chain model is a vector random variable whose components correspond to the individual observations contributed by the cognitive radio receivers.

Another interesting research area is online estimation of the model parameter. In general, the model parameter is estimated offline during the training phase in order to minimize the computation time for the parameter estimation algorithm. If the transmission behavior of the primary user does not vary with time, the parameter estimated offline should be adequate for detection and prediction purposes. However, if the transmission pattern does vary with time, the parameter estimate should be updated periodically by incorporating new observations into the current estimate. This requires a new estimation algorithm that can perform the updating quickly without putting a burden on the processing time.

Appendix A: An Appendix

A.1 Background on the Discrete Phase-Type Distribution

Consider a discrete-time Markov chain $\{X_n\}$ with $r+1$ states $\{1, \ldots, r+1\}$. States $1, \ldots, r$ are transient states and called *phases*, while state $r+1$ is an absorbing state. The transition probability matrix is given by

$$P = \begin{bmatrix} V & \boldsymbol{w} \\ \mathbf{0} & 1 \end{bmatrix}, \tag{A.1}$$

where $\mathbf{0}$ is a row vector of zeros, V is an $r \times r$ matrix, and $\boldsymbol{w}$ is an $r \times 1$ column vector such that

$$V\mathbf{1} + \boldsymbol{w} = \mathbf{1}. \tag{A.2}$$

Note that the transition probability matrix P is completely characterized by the submatrix V. Let $\boldsymbol{u}$ denote a $1 \times r$ row vector representing a probability distribution on $\{1, \ldots, r\}$. Let T denote the time to absorption of the Markov chain $\{X_n\}$ with initial distribution given by $\boldsymbol{u}$. Then T is said have the discrete phase-type distribution with r phases and parameter $(\boldsymbol{u}, V)$ [26]. The probability mass function of T is given by

$$p_T(m) = \boldsymbol{u}V^{m-1}\boldsymbol{w}, \qquad m = 1, 2, \ldots. \tag{A.3}$$

The discrete phase-type distribution is a generalization of the geometric distribution. A geometric distribution with parameter $\alpha \in (0, 1)$ may be seen as a phase-type distribution with 1 phase and parameter $(1, \alpha)$. The discrete-time phase-type distribution also generalizes mixtures and convolutions of a finite number of geometric distributions. As such, the discrete phase-type distribution can be used to approximate a large class of discrete probability distributions. Furthermore, the class of discrete phase-type distributions is dense in the set of all distributions of discrete nonnegative random variables [26].

A.2 Estimated Transition Matrix of the High Order Hidden Bivariate Markov Chain

Since the estimated transition matrix G is a large matrix of size 20×20, we express it in smaller $r \times r$ $(r = 10)$ block matrices $G_{ab}, a, b \in \mathbb{X}$ as follows:

$$G_{11} = \begin{bmatrix} 0.0000 & 0.2568 & 0.4256 & 0.0000 & 0.0709 & 0.0000 & 0.1027 & 0.0000 & 0.1226 & 0.0000 \\ 0.0000 & 0.0000 & 0.0000 & 0.0000 & 0.0000 & 0.0000 & 0.0000 & 0.0000 & 0.0000 & 0.0000 \\ 0.0000 & 0.0000 & 0.0000 & 0.0000 & 0.0000 & 0.0000 & 0.0000 & 0.0000 & 0.0000 & 0.0000 \\ 0.0005 & 0.1505 & 0.1985 & 0.0000 & 0.0652 & 0.1775 & 0.1547 & 0.0154 & 0.0176 & 0.2195 \\ 0.0000 & 0.0000 & 0.0000 & 0.0000 & 0.0000 & 0.0000 & 0.0000 & 0.0000 & 0.0000 & 0.0000 \\ 0.0000 & 0.0094 & 0.0580 & 0.0000 & 0.0005 & 0.0000 & 0.1694 & 0.0000 & 0.0033 & 0.0000 \\ 0.0000 & 0.0000 & 0.0000 & 0.0000 & 0.0000 & 0.0000 & 0.0000 & 0.0000 & 0.0000 & 0.0000 \\ 0.0000 & 0.1171 & 0.3370 & 0.0000 & 0.1534 & 0.0000 & 0.1791 & 0.0000 & 0.0841 & 0.0000 \\ 0.0000 & 0.0000 & 0.0000 & 0.0000 & 0.0000 & 0.0000 & 0.0000 & 0.0000 & 0.0000 & 0.0000 \\ 0.0000 & 0.0353 & 0.4173 & 0.0000 & 0.0512 & 0.0000 & 0.4628 & 0.0000 & 0.0059 & 0.0000 \end{bmatrix}$$

$$G_{12} = \begin{bmatrix} 0.0214 & 0.0000 & 0.0000 & 0.0000 & 0.0000 & 0.0000 & 0.0000 & 0.0000 & 0.0000 & 0.0000 \\ 0.9008 & 0.0031 & 0.0000 & 0.0000 & 0.0210 & 0.0000 & 0.0359 & 0.0000 & 0.0001 & 0.0390 \\ 0.9685 & 0.0003 & 0.0000 & 0.0000 & 0.0032 & 0.0000 & 0.0131 & 0.0000 & 0.0000 & 0.0148 \\ 0.0004 & 0.0000 & 0.0000 & 0.0000 & 0.0000 & 0.0000 & 0.0000 & 0.0000 & 0.0000 & 0.0000 \\ 0.9146 & 0.0046 & 0.0000 & 0.0000 & 0.0455 & 0.0000 & 0.0021 & 0.0000 & 0.0000 & 0.0332 \\ 0.7594 & 0.0000 & 0.0000 & 0.0000 & 0.0000 & 0.0000 & 0.0000 & 0.0000 & 0.0000 & 0.0000 \\ 0.9988 & 0.0000 & 0.0000 & 0.0000 & 0.0001 & 0.0000 & 0.0002 & 0.0000 & 0.0000 & 0.0009 \\ 0.0057 & 0.0000 & 0.0000 & 0.0000 & 0.1228 & 0.0000 & 0.0003 & 0.0000 & 0.0000 & 0.0005 \\ 1.0000 & 0.0000 & 0.0000 & 0.0000 & 0.0000 & 0.0000 & 0.0000 & 0.0000 & 0.0000 & 0.0000 \\ 0.0165 & 0.0000 & 0.0000 & 0.0000 & 0.0106 & 0.0000 & 0.0002 & 0.0000 & 0.0000 & 0.0001 \end{bmatrix}$$

$$G_{21} = \begin{bmatrix} 0.0000 & 0.0000 & 0.0000 & 0.0000 & 0.0000 & 0.0000 & 0.0000 & 0.0000 & 0.0000 & 0.0000 \\ 0.0000 & 0.0000 & 0.0000 & 0.0000 & 0.0000 & 0.0000 & 0.0000 & 0.0000 & 0.0000 & 0.0000 \\ 0.0000 & 0.0000 & 0.0000 & 0.0374 & 0.0000 & 0.0000 & 0.0000 & 0.0000 & 0.0000 & 0.0000 \\ 0.0003 & 0.0000 & 0.0000 & 0.0209 & 0.0000 & 0.0000 & 0.0000 & 0.0003 & 0.0000 & 0.0000 \\ 0.0000 & 0.0000 & 0.0000 & 0.0000 & 0.0000 & 0.0000 & 0.0000 & 0.0000 & 0.0000 & 0.0000 \\ 0.2162 & 0.0005 & 0.0003 & 0.0024 & 0.0003 & 0.0057 & 0.0001 & 0.3794 & 0.0001 & 0.1558 \\ 0.0000 & 0.0000 & 0.0000 & 0.0000 & 0.0000 & 0.0000 & 0.0000 & 0.0000 & 0.0000 & 0.0000 \\ 0.1308 & 0.0111 & 0.0469 & 0.0000 & 0.0207 & 0.3077 & 0.1174 & 0.0202 & 0.2828 & 0.0460 \\ 0.0060 & 0.0000 & 0.0000 & 0.0000 & 0.0000 & 0.0000 & 0.0000 & 0.0000 & 0.0000 & 0.0000 \\ 0.0000 & 0.0000 & 0.0000 & 0.0000 & 0.0000 & 0.0000 & 0.0000 & 0.0000 & 0.0000 & 0.0000 \end{bmatrix}$$

$$G_{22} = \begin{bmatrix} 0.0000 & 0.0330 & 0.0002 & 0.0000 & 0.0253 & 0.0000 & 0.1454 & 0.0000 & 0.0007 & 0.7955 \\ 0.0000 & 0.0000 & 0.9568 & 0.0244 & 0.0000 & 0.0007 & 0.0000 & 0.0008 & 0.0173 & 0.0000 \\ 0.0000 & 0.0000 & 0.0000 & 0.8899 & 0.0000 & 0.0624 & 0.0000 & 0.0102 & 0.0000 & 0.0000 \\ 0.0008 & 0.0000 & 0.0000 & 0.0000 & 0.0000 & 0.7156 & 0.0000 & 0.2620 & 0.0000 & 0.0000 \\ 0.0000 & 0.0000 & 0.9349 & 0.0001 & 0.0000 & 0.0000 & 0.0000 & 0.0000 & 0.0651 & 0.0000 \\ 0.0345 & 0.0000 & 0.0000 & 0.0000 & 0.0000 & 0.0000 & 0.0000 & 0.2046 & 0.0000 & 0.0001 \\ 0.0000 & 0.2868 & 0.1008 & 0.0282 & 0.1979 & 0.0004 & 0.0000 & 0.0000 & 0.3859 & 0.0000 \\ 0.0056 & 0.0001 & 0.0000 & 0.0000 & 0.0042 & 0.0000 & 0.0036 & 0.0000 & 0.0000 & 0.0030 \\ 0.0000 & 0.0000 & 0.0510 & 0.8746 & 0.0000 & 0.0021 & 0.0000 & 0.0663 & 0.0000 & 0.0000 \\ 0.0000 & 0.5373 & 0.0547 & 0.0047 & 0.0915 & 0.0151 & 0.0000 & 0.0000 & 0.2966 & 0.0000 \end{bmatrix}$$

Bibliography

Bibliography

[1] I. A. Akbar and W. H. Tranter. Dynamic spectrum allocation in cognitive radio using hidden Markov models: Poisson distributed case. *Proceedings of IEEE Southeast Conference*, pages 196–201, March 2007.

[2] L. E. Baum, T. Petrie, G. Soules, and N. Weiss. A maximization technique occuring in the statistical analysis of probabilistic functions of Markov chains. *The Annals of Mathematical Statistics*, 41(1):164–171, 1970.

[3] D. R. Brillinger. *Time Series: Data Analysis and Theory.* Holt, Rinehart, and Winston, New York, 1975.

[4] R. W. Chang and J. C. Hancock. On receiver structures for channels having memory. *IEEE Trans. Information Theory*, IT-12:463–468, October 1966.

[5] Z. Chen, N. Guo, Z. Hu, and R. C. Qiu. Channel state prediction in cognitive radio, Part II: Single-user prediction. *Proceedings of IEEE SoutheastCon*, pages 50–54, March 2011.

[6] Z. Chen, N. Guo, Z. Hu, and R. C. Qiu. Experimental validation of channel state prediction considering delays in practical cognitive radio. *IEEE Transactions on Vehicular Technology*, 60:1314–1325, May 2011.

[7] City-Data. Tysons Corner, Virginia. `http://www.city-data.com/city/Tysons-Corner-Virginia.html`.

[8] T. C. Clancy and B. D. Walker. Predictive dynamic spectrum access. *Proceedings SDR Forum Technical Conference*, November 2006.

[9] C. Cordeiro, M. Ghosh, D. Cavalcanti, and K. Challapali. Spectrum sensing for dynamic spectrum access of tv bands. *Cognitive Radio Oriented Wireless Networks and Communications (CrownCom) Conference*, pages 225–233, August 2007.

[10] A. P. Dempster, N. M. Laird, and D. B. Rubin. Maximum likelihood from incomplete data via the EM algorithm. *Royal Statistical Society*, 39(1):1–38, 1977.

[11] T. Do and B. L. Mark. Joint spatial-temporal spectrum sensing for cognitive radio networks. *IEEE Trans. on Vehicular Technology*, 59(7):3480–3490, Sept. 2010.

[12] Y. Ephraim and N. Merhav. Hidden Markov processes. *IEEE Transactions on Information Theory*, 48(6):1518–1569, June 2002.

[13] FCC. Paging band plan. http://wireless.fcc.gov/services/index.htm.

[14] FCC. Universal licensing system. http://wireless2.fcc.gov/UlsApp/UlsSearch/searchLicense.jsp.

[15] FCC. White space database administration. http://www.fcc.gov/encyclopedia/white-space-database-administration.

[16] FCC Spectrum Policy Task Force. Report of the spectrum efficiency working group. Technical report, November 2002.

[17] S. Geirhofer, L. Tong, and B. M. Sadler. A measurement-based model for dynamic spectrum access in WLAN channels. *Proceedings IEEE Military Communication Conference*, pages 1–7, Oct. 2006.

[18] S. Geirhofer, L. Tong, and B. M. Sadler. Dynamic spectrum access in the time domain: Modeling and exploiting white space. *IEEE Communications Magazine*, 45:66–72, May 2007.

[19] C. Ghosh, C. Cordeiro, D. P. Agrawal, and M. B. Rao. Markov chain existence and hidden Markov models in spectrum sensing. *IEEE Pervasive Computing and Communications*, pages 1–6, March 2009.

[20] R. M. Gray and L. D. Davisson. *An Introduction to Statistical Signal Processing*. Cambridge University Press, 2004.

[21] G. Grimmett and D. Stirzaker. *Probability and Random Processes*. Oxford University Press, New York, third edition, 2001.

[22] K. Haghighi, E. G. Strom, and E. Agrell. On optimum causal cognitive spectrum reutilization strategy. *IEEE Journal on Selected Areas in Communications*, 30:1911–1921, November 2012.

[23] S. Haykin. Cognitive radio: Brain-empowered wireless communications. *IEEE Journal on Selected Areas in Communications*, 23:201–220, February 2005.

[24] A. He and et al. A survey of artificial intelligence for cognitive radios. *IEEE Transactions on Vehicular Technology*, 59:1578–1592, May 2010.

[25] IEEE Dynamic Spectrum Access Networks (DySPAN). http://www.ieee-dyspan.org.

[26] G. Latouche and V. Ramaswami. *Introduction to matrix analytic methods in stochastic modeling*. ASA/SIAM Series on Statistics and Applied Probability, 1999.

[27] B. L. Mark and Y. Ephraim. An EM algorithm for continuous-time bivariate Markov chains. *Computational Statistics and Data Analysis*, 57(1):504–517, January 2013.

[28] B. L. Mark and A. O. Nasif. Estimation of maximum interference-free transmit power level for opportunistic spectrum access. *IEEE Trans. on Wireless Communications*, 8(5):2505–2513, May 2009.

[29] J. W. Mark and W. Zhuang. *Wireless Communications and Networking*. Prentice Hall, New Jersey, 2002.

[30] R. Min, D. Qu, Y. Cao, and G. Zhong. Interference avoidance based on multi-step-ahead prediction for cognitive radio. *Conference on Communication Systems (ICCS)*, pages 227–231, November 2008.

[31] J. Mitola. Cognitive radio for flexible mobile multimedia communications. *IEEE International Workshop on Mobile Multimedia Communications*, pages 3–10, 1999.

[32] T. Nguyen, B. L. Mark, and Y. Ephraim. Hidden Markov process based dynamic spectrum access for cognitive radio. *Conference on Information Sciences and Systems (CISS)*, pages 1–6, March 2011.

[33] T. Nguyen, B. L. Mark, and Y. Ephraim. Spectrum sensing using a hidden bivariate Markov chain model. *submitted to IEEE Trans. on Wireless Communications*, November 2012.

[34] C.-H. Park, S.-W. Kim, S.-M. Lim, and M.-S. Song. HMM based channel status predictor for cognitive radio. *Asia-Pacific Microwave Conference*, pages 1–4, December 2007.

[35] W. J. J. Roberts and Y. Ephraim. An EM algorithm for ion-channel current estimation. *IEEE Transactions on Signal Processing*, 56(1):26–33, January 2008.

[36] SDR Forum. Use cases for MLM language in modern wireless networks. Technical report, January 2009.

[37] Shared Spectrum Company. General survey of radio frequency bands: 30 MHz to 3 GHz. Technical report, August 2010.

[38] SRI XG Team. Next generation communication. `http://xg.csl.sri.com`.

[39] Z. Sun, G. Bradford, and N. Laneman. Sequence detection algorithms for PHY-layer sensing in dynamic spectrum access networks. *IEEE Journal on Selected Topics in Signal Processing*, 5(1):97–109, February 2011.

[40] K. W. Sung, S.-L. Kim, and J. Zander. Temporal spectrum sharing based on primary user activity prediction. *IEEE Transactions on Wireless Communications*, 9(12):3848–3855, December 2010.

[41] H. Tang. Some physical layer issues of wide-band cognitive radio systems. *IEEE Proceedings Dynamic Spectrum Access Networks (DySPAN)*, pages 151–159, November 2005.

[42] J. Unnikrishnan and V. Veeravalli. Cooperative sensing for primary detection in cognitive radio. *IEEE Journal Sel. Topics Signal Process.*, 2(1):18–27, Feb. 2008.

[43] Virginia Tech Center for Wireless Telecommunications (CWT). `http://www.cognitiveradio.wireless.vt.edu/dokuwiki/doku.php?id=home`.

[44] W. Wei, B. Wang, and D. Towsley. Continuous-time hidden Markov models for network performance evaluation. *Elsevier Science, Performance Evaluation*, 49:129–146, September 2002.

[45] Wireless Innovation Forum. `http://www.wirelessinnovation.org`.

[46] Y. Xing. Cognitive radio networks: Learning, games and optimization. *PhD. Dissertation*, 2006.

[47] S. Z. Yu. Hidden Semi-Markov Models. *Artificial Intelligence*, 174:215–243, 2010.

[48] T. Yucek and H. Arslan. A survey of spectrum sensing algorithms for cognitive radios applications. *IEEE Communications Surveys and Tutorials*, 11:116–130, 2009.

[49] Q. Zhao, S. Geirhofer, L. Tong, and B. M. Sadler. Optimal dynamic spectrum access via periodic channel sensing. *IEEE Wireless Communications and Networking Conference*, pages 33–37, March 2007.

[50] Q. Zhao, S. Geirhofer, L. Tong, and B. M. Sadler. Opportunistic spectrum access via periodic channel sensing. *IEEE Transactions on Signal Processing*, 56(2):785–796, February 2008.

[51] Q. Zhao and B. M. Sadler. A survey of dynamic spectrum access: Signal processing, networking, and regulatory policy. *IEEE Signal Processing Magazine*, 24:79–89, May 2007.

[52] Q. Zhao, L. Tong, A. Swami, and Y. Chen. Decentralized cognitive MAC for opportunistic spectrum access in ad hoc networks: A POMDP framework. *IEEE Journal on Selected Areas in Communications.*, 25:589–600, April 2007.

Curriculum Vitae

Thao Tran Nhu Nguyen was born in Chau Doc, An Giang, Vietnam. She moved to Ho Chi Minh city to attend Le Hong Phong high school for the Gifted. After graduating high school, she came to the U.S. as an exchange student and finished her AS at the Wabash Valley College in Illinois (Summa Cum Laude). She continued her education and obtained her BS, MS, and PhD, all in Electrical Engineering, at George Mason University in 2004, 2006, and 2013, respectively, all with great honors (Magna Cum Laude). Her dissertations title is "Hidden Markov model based spectrum sensing for cognitive radio", which was under the advice of both Professor Brian L. Mark and Professor Yariv Ephraim. While working on her MS and PhD, she continued working full time as an engineer at Shared Spectrum Company (SSC). Her main topics of interest are wireless communications, especially cognitive radio applications, and signal processing.